Chapter 0.1
THREE-NUCLEON SCATTERING

W. Glöckle
Ruhr-Universität Bochum,
Institut für theoretische Physik II,
44780 Bochum
Germany

SCATTERING IN MICROSCOPIC PHYSICS AND CHEMICAL PHYSICS
Three-Nucleon Scattering

Contents

0.1.1. Introduction

Nucleon scattering on very light nuclei is an ideal laboratory to test nuclear forces and reaction theory. The first nontrivial system consists of three nucleons (3N) and is of specific interest, since it can be solved exactly on todays supercomputers[1]. Additionally, here three-nucleon forces (3NF) appear for the first time. Knowledge about nature and size of the 3NF is of fundamental importance for nuclear physics. The next step to the system with four nucleons has not yet been fully accomplished. While the 4N bound state can already be solved exactly[2,3,4], 4N scattering has not yet been mastered. However, investigations within limited energy ranges as well as based in part on simplified nuclear forces exist[5]. When considering todays modern 3N calculations, where realistic nuclear forces in all their complexities can be handled numerically exactly, one has to remember that there was a long evolution from the first model calculations[23] of three-body systems to today's standards[1]. We would like to refer to the review article[1] for more detailed information about the many intermediate steps.

Here we concentrate on 3N scattering formulated in the Faddeev scheme[6]. In Section 0.1.2 the basic formalism is laid out. The specific form of Faddeev equations most suited for numerical investigations in momentum space is derived in Section 0.1.3. A closely related formalism illustrating the variety of possible approaches is displayed in Section 0.1.4. The rich set of spin observables is described in Section 0.1.5. A brief insight into the actual algebraic preparations necessary for the numerical implementation is given in Section 0.1.6. The dynamical input for 3N-calculations is presented in Section 0.1.7. Very recent results based on modern NN and 3NF's are shown in Section 0.1.8. This illustrates successes and failures in our present day understanding of nuclear dynamics in the 3N system. We conclude with an outlook in Section 0.1.9.

0.1.2. Basic scattering formalism

In 3N scattering there are two asymptotic geometrical configurations: two- and three-body fragmentations. In the usual experimental set up the scattering process is initiated by a two-body fragmentation, i.e. a nucleon hits a deuteron. This particular fragmentation is governed by the channel Hamiltonian

$$H_i = H_0 + V_i, \tag{1}$$

where H_0 is the kinetic energy operator. The pair interaction is denoted by the convenient "odd man out" notation

$$V_i \equiv V_{jk},\ j,k \neq i. \tag{2}$$

The initial configuration shall be described by the wavepacket

$$|\Phi_i(t)\rangle = \int d\vec{q}\,|\Phi_{\vec{q}}\rangle_i e^{-iE_q t}\ f(\vec{q}), \tag{3}$$

which is a solution of the time-dependent Schrödinger equation

$$H_i|\Phi_i(t)\rangle = \frac{1}{i}\frac{\partial}{\partial t}|\Phi_i(t)\rangle \tag{4}$$

The state entering Eq.(3) is given by

$$|\ \Phi_{\vec{q}}\rangle_i\ = |\ \phi_d\rangle_{jk}\ |\ \vec{q}\rangle_i \tag{5}$$

and is an eigenstate to H_i:

$$H_i|\Phi_{\vec{q}}\rangle_i = E_{\vec{q}_i}|\Phi_{\vec{q}}\rangle_i. \tag{6}$$

The indices at the ket vectors in Eq.(5) refer to the particle numbers. Thus the two-nucleon bound state,

the deuteron, is composed of nucleons j and k and the projectile nucleon i is described by its Jacobi momentum $\vec{q}$. One has

$$E_{\vec{q}} = E_d + \frac{3}{4m}\ \vec{q}^{\,2} \tag{7}$$

where $E_d < 0$ is the deuteron binding energy and m the nucleon mass. The Jacobi momenta will be defined in Eqs.(44 - 45). Finally $f(\vec{q})$ is a square integrable momentum distribution, which provides the shape of the free wavepacket in the distant past.

The full scattering state $\Psi_i^{(+)}(t)$ develops out of the state $\Phi_i(t)$. As is well known, the matching condition has to be chosen to be

$$\lim_{t\to-\infty} \parallel \Psi_i^{(+)}(t) \ - \ \Phi_i(t) \parallel \ = \ 0 \tag{8}$$

This is equivalent to

$$\lim_{t\to-\infty} \parallel \Psi_i^{(+)}(0) \ - \ e^{iHt}\ e^{-iH_it}\ \phi_i(0) \parallel = 0 \tag{9}$$

where H is the full Hamiltonian

$$H \ = \ H_0 + \sum_{i=1}^{3} V_i + V_4 \tag{10}$$

It is composed of the kinetic energy H_0, the three pair interactions V_i and the 3NF V_4. Eq.(9) leads to the explicit expression for the scattering state at time $t = 0$

$$\Psi_i^{(+)}(0) \ = \ \lim_{\tau\to-\infty}\ e^{iH\tau}\ e^{-iH_i\tau}\ \phi_i(0) \tag{11}$$

For strong interactions, which are short ranged, this limit exists. The proof follows closely the one for potential scattering[7]. In a well known manner Eq.(11) can be reformulated using Eqs.(3) and (6) as

$$\begin{aligned}\Psi_i^{(+)}(0) &= \lim_{\varepsilon\to0}\ \varepsilon \int_{-\infty}^{0} d\tau e^{\varepsilon\tau}\ e^{iH\tau}e^{-iH_i\tau}\phi_i(0) \\ &= \lim_{\varepsilon\to0}\ \varepsilon \int_{-\infty}^{0} d\tau \int d\vec{q} e^{i(H-E_{\vec{q}}-i\varepsilon)\tau}\Phi_{\vec{q}}\ f(\vec{q}) \\ &= \lim_{\varepsilon\to0} \int d\vec{q} \frac{i\varepsilon}{E_q + i\varepsilon - H}\Phi_{\vec{q}} f(\vec{q})\end{aligned} \tag{12}$$

We define the state

$$\Psi_{\vec{q}}^{(+)} \ \equiv \ \lim_{\varepsilon\to0}\ \frac{i\varepsilon}{E_q + i\varepsilon - H}\ \Phi_{\vec{q}}, \tag{13}$$

which is a solution of the stationary 3N Schrödinger equation

$$H|\Psi_{\vec{q}}^{(+)}\rangle = \ E_q|\Psi_{\vec{q}}^{(+)}\rangle \tag{14}$$

It should be noted that the expression given in Eq.(13) incorporates all the boundary conditions, though not yet in a manifest form. When inserting the definition given in Eq.(13) into Eq.(12) one yields the transparent form

$$\Psi_i^{(+)}(0) \ = \ \int d\vec{q}\ \Psi_{\vec{q}}^{(+)} f(\vec{q}) \tag{15}$$

which describes the time-dependent scattering state (at time $t = 0$) as a superposition of the specific eigenstates $\Psi_{\vec{q}}^{(+)}$ of H according to the initial momentum distribution. It follows that at an arbitrary time $\Psi_i^{(+)}(t)$ is given as

$$\Psi_i^{(+)}(t) \ = \ e^{-iHt}\ \Psi_i^{(+)}(0) \ = \ \int d\vec{q}\ e^{-iEqt}\ \Psi_{\vec{q}}^{(+)} f(\vec{q}) \tag{16}$$

In order to keep the notation concise it is advisable to introduce at an early stage the indistinguishability of the nucleons by using the isospin formalism. Equipped with the isospin label the nucleons can be considered to be identical. The state $\Psi_i^{(+)}(t)$ given in Eq.(16) is antisymmetric only under exchange of nucleons j and k. This follows from Eq.(13) if the deuteron state in $\Phi_{\vec{q}}$ is chosen to be antisymmetric. The Hamiltonian H is a symmetric operator, thus the antisymmetrization in the nucleons numbered j and k carries over to the state $\Psi_q^{(+)}$. We now introduce cyclic and anticyclic permutation and define

$$1 \ + \ P \ \equiv \ 1 + \ P_{ij}\ P_{jk} \ + \ P_{ik}\ P_{jk} \tag{17}$$

This applied onto $\Psi_i^{(+)}(t)$ gives

$$\begin{aligned}|\ \Psi_a^{(+)}(t)\rangle \ &\equiv (1+P)\ |\ \Psi_i^{(+)}(t)\rangle \\ &= \int d\vec{q}\ f(\vec{q}) e^{-iEqt}\ |\ \Psi_{\vec{q}}^{(+)}\rangle_a,\end{aligned} \tag{18}$$

where

$$\begin{aligned}|\ \Psi_{\vec{q}}^{(+)}\rangle_a \ &\equiv \ (1+P)\ |\ \Psi_{\vec{q}}^{(+)}\rangle \\ &\equiv \ |\ \Psi_{\vec{q}}^{(+)}\rangle_1 + \ |\ \Psi_{\vec{q}}^{(+)}\rangle_2 + |\ \Psi_{\vec{q}}^{(+)}\rangle_3\end{aligned} \tag{19}$$

We introduced indices on the ket vectors. Their obvious meaning is that for instance $|\ \Psi_{\vec{q}}^{(+)}\rangle_1$ denotes the scattering state, in which the asymptotic initial momentum $\vec{q}$ is carried by nucleon 1, and the initial asymptotic deuteron is formed out of nucleons 2 and 3. The two other states result by a cyclic and an anticyclic permutation of the three nucleons. It is a simple exercise to verify that $|\ \Psi_a^{(+)}(t)\rangle$ is antisymmetric under all transpositions P_{kl}.

After the scattering process the three nucleons separate again into three two-body fragmentations (one elastic and two rearrangement scatterings) and a three-body fragmentation (breakup scattering). A two-body fragmentation with a sharp relative momentum $\vec{q}_f$ is described by

$$\phi_{\vec{q}_f}(t) \ = \ e^{-iEq_ft}\phi_{\vec{q}_f} \tag{20}$$

and the 3-body fragmentation with sharp relative momenta $\vec{p}_f$ and $\vec{q}_f$ by

$$\phi_{\vec{p}_f\vec{q}_f}(t) \;=\; e^{-iE_{\vec{p}_f\vec{q}_f}t}\phi_{\vec{p}_f\vec{q}_f} \;\equiv\; e^{-iE_{\vec{p}_f\vec{q}_f}\;t}\mid \vec{p}_f\vec{q}_f\rangle \quad (21)$$

The transition amplitudes at time t from the two-body fragmentation defined by the initial momentum distribution $f(\vec{q})$ into the states $\phi_{\vec{q}_f}(t)$ or $\phi_{\vec{p}_f\vec{q}_f}(t)$ are given as

$$A_{\vec{q}_f}(t) \;\equiv\; \langle\phi_{\vec{q}_f}\;(t)\;\mid\;\Psi_a^{(+)}(t)\rangle \quad (22)$$

$$A_{\vec{p}_f\vec{q}_f}(t) \;\equiv\; \langle\phi_{\vec{p}_f\;\vec{q}_f}\;(t)\;\mid\;\Psi_a^{(+)}(t)\rangle \quad (23)$$

The stationary scattering state $\mid\;\Psi_{\vec{q}}^{(+)}\rangle_1$ defined by Eq.(13) obeys the triad of Lippmann Schwinger (L.S.) equations[7,8]

$$\begin{aligned}
&|\Psi_{\vec{q}}^{(+)}\rangle_1 \\
&= \mid\phi_{\vec{q}}\rangle_1 + \frac{1}{E_{\vec{q}}+i\epsilon-H_1}\;(V_2+V_3+V_4)\mid\Psi_{\vec{q}}^{(+)}\rangle_1 \quad (24)\\
&= \frac{1}{E_{\vec{q}}+i\epsilon-H_2}\;(V_3+V_1+V_4)\mid\Psi_{\vec{q}}^{(+)}\rangle_1 \quad (25)\\
&= \frac{1}{E_{\vec{q}}+i\epsilon-H_3}\;(V_1+V_2+V_4)\mid\Psi_{\vec{q}}^{(+)}\rangle_1 \quad (26)
\end{aligned}$$

This set of three Lippmann Schwinger equations defines the scattering state $\mid\;\Psi_{\vec{q}}^{(+)}\rangle_1$ uniquely (see Section 0.1.4). As a consequence $\mid\;\Psi_{\vec{q}}^{(+)}\rangle_2$ and $\mid\;\Psi_{\vec{q}}^{(+)}\rangle_3$ will obey the homogeneous version of the first L.S. equation given in Eq.(24), and therefore $\mid\;\Psi_{\vec{q}}^{(+)}\rangle_a$ defined in Eq.(19) is also a solution of that first equation in the triad. Because of the antisymmetrization of $\mid\;\Psi_{\vec{q}}^{(+)}\rangle_a$ it does not matter how the nucleons are numbered in the state $\phi_{\vec{q}_f}(t)$ of Eq.(20). It is convenient to choose $\mid\phi_{\vec{q}_f}\rangle_1$. Then it follows immediately from Eqs.(22), (18), and (24) that

$$\begin{aligned}
A_{\vec{q}_f}(t) \;=\;& f(\vec{q}_f) + \int d\vec{q}\;e^{\,i(E_{\vec{q}_f}-E_{\vec{q}})t}\;\frac{1}{E_{\vec{q}}+i\epsilon-E_{\vec{q}_f}}\\
&\langle\phi_{\vec{q}_f}\;\mid V_2+V_3+V_4\;\mid\;\Psi_{\vec{q}}^{(+)}\rangle_a\;f(\vec{q}) \quad (27)
\end{aligned}$$

The evaluation of the cross section requires the knowledge of the transition rate $\frac{d}{dt}\mid A_{\vec{q}_f}(t)\mid^2$ for $t\to\infty$. Since $\mid\;\Psi_a^{(+)}(t)\rangle$ for $t\to\infty$ separates into free motions of two- and three-body fragmentations $A_{\vec{q}_f}(t)$ has to go towards a time-independent limit for $t\to\infty$, and consequently the transition rate has to vanish in that limit. Only together with an increasingly sharper initial wave packet centered around an initial momentum $\vec{q}_0$the ratio of the transition rate to the incoming flux approaches a nonzero value, which moreover will be independent of the shape $f(\vec{q})$ of the initial momentum distribution. This last property is of course a necessary requirement to gain information on the dynamics in the scattering process without disturbance through the initial form of the wavepacket (which would be anyhow uncontrollable).

Since the form of $f(\vec{q})$ should and does not matter we can use e.g. a Gaussian distribution, which has a simple connection to a sequence of functions $f_\delta(\vec{q})$ defining a δ-function in the limit $b\to 0$:

$$f(\vec{q}) \;=\; b^{3/4}(2\pi)^{3/4}f_\delta(\vec{q}) \quad (28)$$

$$f_\delta(\vec{q}) \;=\; \frac{1}{b^3}\frac{1}{(\pi)^{3/2}}\;e^{(\vec{q}-\vec{q}_0)^2/b^2} \quad (29)$$

Note that $f(\vec{q})$ should not tend towards a delta function, since it should be square integrable. The choice (28) and (29) guarantees for $b\neq 0$

$$\int d\vec{q}\;\mid f(\vec{q})\mid^2 = 1, \quad (30)$$

and

$$f_\delta(\vec{q}) \;\xrightarrow[b\to 0]{}\; \delta(\vec{q}-\vec{q}_0) \quad (31)$$

Simple algebra[1] leads then in the limit $b\to 0$ to

$$\begin{aligned}
&\lim_{b\to 0}\;\frac{1}{b^3(2\pi)^{3/2}}\;\frac{d}{dt}\mid A_{\vec{q}_f}(t)\mid^2\\
&\quad= 2Im\langle\phi_{\vec{q}_f}\mid U\mid\phi_{\vec{q}_0}\rangle\delta(\vec{q}_f-\vec{q}_0) \quad (32)\\
&\qquad+2\pi\;\delta(E_{\vec{q}_0}-E_{\vec{q}_f})\;\mid\langle\phi_{\vec{q}_f}\;\mid U\;\mid\;\phi_{\vec{q}_0}\rangle\mid^2
\end{aligned}$$

with

$$\begin{aligned}
&\langle\phi_{\vec{q}_f}\;\mid\;U\;\mid\;\phi_{\vec{q}_0}\rangle \quad (33)\\
&\equiv\; {}_1\langle\phi_{\vec{q}_f}\;\mid\;V_2+V_3+V_4\;\mid\;\Psi_{\vec{q}_0}^{(+)}\rangle_a
\end{aligned}$$

The initial current $\mid\;\vec{j}\;\mid$ carries the same factor $b^3(2\pi)^{3/2}$ in the limit $b\to 0$ as follows from Eq.(3), and one has

$$\mid\vec{j}\mid \;=\; b^3(2\pi)^{3/2}\;\frac{3}{2m}\frac{\mid\vec{q}_0\mid}{(2\pi)^3} \quad (34)$$

$$\equiv\; b^3(2\pi)^{3/2}\mid\vec{j}_0\mid \quad (35)$$

As a consequence the differential cross section for elastic nucleon-deuteron scattering turns out to be

$$d\sigma = \frac{1}{\mid\vec{j}_0\mid}\int d\vec{q}_f 2\pi\delta(E_{\vec{q}_0}-E_{\vec{q}_f})\mid\langle\phi_{\vec{q}_f}\mid U\mid\phi_{\vec{q}_0}\rangle\mid^2 \quad (36)$$

or

$$\frac{d\sigma}{d\hat{q}_f} \;=\; (\frac{2}{3}m)^2\;(2\pi)^4\;\mid\langle\phi_{\vec{q}_f}\;\mid U\;\mid\;\phi_{\vec{q}_0}\rangle\mid^2 \quad (37)$$

Thus Eq.(33) defines the operator U for elastic scattering acting between the "channel states" $\phi_{\vec{q}}$ given in Eq.(5)

The derivation of the break-up cross section follows similar steps, and starts with the transition amplitude given in Eq.(23). Here we use the fact that every stationary scattering state initiated in a two-body fragmentation channel obeys the homogeneous

equation, where the free 3N propagator enters the integral kernel. Therefore we can use

$$\mid \Psi^{(+)}_{\vec{q}} \rangle_a \;=\; \frac{1}{E_{\vec{q}} + i\epsilon - H_0}\;(V_1 + V_2 + V_3 + V_4)\;\mid \Psi^{(+)}_{\vec{q}} \rangle_a \tag{38}$$

in Eq.(18) and Eq.(23) and obtain the result

$$A_{\vec{p}_f \vec{q}_f}(t) = \int d\vec{q}\;\frac{e^{i(E_{\vec{p}_f\vec{q}_f} - E_{\vec{q}})t}}{E_{\vec{q}} - E_{\vec{p}_f\vec{q}_f} + i\epsilon} \tag{39}$$
$$\langle \phi_{\vec{p}_f\vec{q}_f} \;\mid\; V_1 + V_2 + V_3 + V_4 \;\mid \Psi^{(+)}_{\vec{q}} \rangle_a \; f(\vec{q})$$

Similar steps to those for obtaining $A_{\vec{q}_f}(t)$ lead to

$$\lim_{b\to o}\;\frac{1}{b^3(2\pi)^{3/2}}\;\frac{d}{dt}\;\mid\; A_{\vec{p}_f\vec{q}_f}(t)\;\mid^2 \tag{40}$$
$$=\; 2\pi\;\delta(E_{\vec{q}_0} - E_{\vec{p}_f\vec{q}_f})\;\mid\langle\phi_{\vec{p}_f\vec{q}_f}\;\mid\; U_0\;\mid\phi_{\vec{q}_0}\rangle\mid^2$$

where

$$\langle\;\; \phi_{\vec{p}_f\vec{q}_f}\;\mid\; U_0\;\mid\;\phi_{\vec{q}_0}\rangle \tag{41}$$
$$\equiv\; \langle\phi_{\vec{p}_f\vec{q}_f}\;\mid\; V_1 + V_2 + V_3 + V_4\;\mid\;\Psi^{(+)}_{\vec{q}_0}\rangle_a$$

The result is the breakup cross section

$$d\sigma = \frac{1}{\mid \vec{j}_0 \mid}\int d\vec{p}_f\, d\vec{q}_f\;2\pi(E_{\vec{q}_0} - E_{\vec{p}_f\vec{q}_f}) \tag{42}$$
$$\mid\langle\phi_{\vec{p}_f\vec{q}_f}\;\mid U_0\;\mid\phi_{\vec{q}_0}\rangle\;\mid^2$$

We now rewrite this expression into laboratory momenta $\vec{k}_i\;\; i = 1,2,3$ and the initial projectile momentum $\vec{k}_{lab}$:

$$d\sigma = \frac{m}{k_{lab}}(2\pi)^4\;\int d\vec{k}_1\;d\vec{k}_2\;d\vec{k}_3$$
$$\delta(\vec{k}_{lab} - \vec{k}_1 - \vec{k}_2 - \vec{k}_3)$$
$$\delta(E_{lab} + E_d - \sum_{i=1}^{3}\frac{\vec{k}_i^{\,2}}{2m})\;\mid\langle\phi_{\vec{p}_f\vec{q}_f}\;\mid U_0\;\mid\;\phi_{\vec{q}_0}\rangle\mid^2 \tag{43}$$

The Jacobi momenta entering the nuclear matrix element are defined as

$$\vec{p}\;\;=\;\;\frac{1}{2}(\vec{k}_2 - \vec{k}_3) \tag{44}$$
$$\vec{q}\;\;=\;\;\frac{2}{3}(\vec{k}_1 - \frac{1}{2}\;(\vec{k}_2 + \vec{k}_3)) \tag{45}$$

This is one particular choice. The other two possible choices simply follow by a cyclic and anticyclic permutation.

The most detailed break-up cross section results by measuring two nucleons in coincidence. This leads to a fivefold differential cross section

$$\frac{d^5\sigma}{d\hat{k}_1 d\hat{k}_2 dE_1} = (2\pi)^4 m^3\sqrt{2mE_1}k_2^2 \tag{46}$$
$$\frac{\mid\langle\phi_{\vec{p}_f\vec{q}_f}\;\mid U_0\;\mid\phi_{\vec{q}_0}\rangle\mid^2}{k_{lab}\;\mid 2k_2 - (\vec{k}_{lab} - \vec{k}_1)\cdot\hat{k}_2\;\mid}$$

The energy conserving δ-function connects the momentum k_2 of particle 2 to E_1 for given directions $\hat{k}_1$ and $\hat{k}_2$ of the two detected nucleons. This connection defines the kinematical locus on which all events have to be located. In order to avoid the singularity of the denominator in Eq.(46) one replaces the E_1-variable by an arclength S along that kinematical locus which leads to

$$\frac{d^5\sigma}{d\hat{k}_1 d\hat{k}_2 dS} =$$
$$\frac{(2\pi)^4\;\mid\langle\phi_{\vec{p}_f\vec{q}_f}\;\mid U_0\;\mid\phi_{\vec{q}_0}\rangle\mid^2 m^3 k_1^2 k_2^2/k_{lab}}{\sqrt{k_1^2(2k_2 - \hat{k}_2\cdot(\vec{k}_{lab} - \vec{k}_1))^2 + k_2^2(2k_1 - \hat{k}_1\cdot(\vec{k}_{lab} - \vec{k}_2))^2}} \tag{47}$$

In this form the break-up data of Section 0.1.8 will be presented.

Up to now we neglected in the notation spin magnetic quantum numbers. For unpolarized cross sections all the expressions, specifically the final ones of Eqs.(37) and (46) have to be averaged over the initial state and summed over the final state magnetic quantum numbers (see Section 0.1.5).

0.1.3. Dynamical equations in Faddeev form

Equations in which NN forces for each pair of nucleons are summed up to infinite order into NN t-operators can be written down in various forms. Similarly, 3NFs can be incorporated in different manners. Here we present a specific form, which turned out to be most convenient for a numerical treatment in momentum space[9]. The antisymmetrized stationary scattering state given in Eq.(19) obeys the homogeneous equation

$$\mid \Psi^{(+)}_{\vec{q}} \rangle_a \;=\; G_0\;\sum_{i=1}^{4} V_i\;\mid \Psi^{(+)}_{\vec{q}} \rangle_a \tag{48}$$

It is convenient to separate V_4, the 3NF, into three different parts, which is for the currently employed forces quite a natural decomposition, namely

$$V_4\;\equiv\;\sum_{i=1}^{3} V_4^{(i)} \tag{49}$$

The decomposition is such that $V_4^{(i)}$ is symmetric under the exchange of nucleons j and k. In the case of the 2π-exchange 3NF $V_4^{(i)}$ is that part, where the nucleon i undergoes $\pi - N$ (off-the-mass-shell) scattering (see Section 0.1.6). Using Eq.(49) we can rewrite Eq.(48) as

$$\mid \Psi^{(+)}_{\vec{q}} \rangle_a \;=\; G_0\;\sum_{i=1}^{3}(V_i + V_4^{(i)})\;\mid \Psi^{(+)}_{\vec{q}} \rangle_a \tag{50}$$

This defines three Faddeev components,

$$| \Psi_{\vec{q}}^{(+)} \rangle_a \equiv \sum_{i=1}^{3} \psi_i \quad (51)$$

with

$$\psi_i \equiv G_0(V_i + V_4^{(i)}) \mid \Psi_{\vec{q}}^{(+)} \rangle_a \quad (52)$$

Because of the identity of the nucleons the three components ψ_i are identical in their functional form, only the particles are permuted. Thus with the help of the permutation operators given in Eq.(17) one obtains

$$| \Psi_{\vec{q}}^{(+)} \rangle_a = (1+P)\psi_1 \quad (53)$$

It follows

$$\psi_1 = G_0\ V_1(1+P)\psi_1 + G_0\ V_4^{(1)}(1+P)\psi_1 \quad (54)$$

or

$$(1 - G_0\ V_1)\psi_1 = G_0\ V_1\ P\psi_1 + G_0\ V_4^{(1)}(1+P)\psi_1 \quad (55)$$

The boundary condition for the initial channel state $\phi_1 \equiv \mid \phi_{\vec{q}_0} \rangle_1$ can be naturally incorporated noting that according to Eq.(6)

$$(1 - G_0\ V_1)\phi_1 = 0 \quad (56)$$

Further we introduce the NN t-operator through

$$(1 - G_0\ V_1)^{-1} G_0\ V_1 \equiv G_0\ t_1, \quad (57)$$

which is equivalent to the standard Lippmann Schwinger equation

$$t_1 = V_1 + V_1\ G_0\ t_1 \quad (58)$$

The resulting Faddeev equation is given by

$$\psi_1 = \phi_1 + G_0\ t_1 P\psi_1 + (1 + G_0\ t_1) G_0\ V_4^{(1)}(1+P)\psi_1 \quad (59)$$

The homogeneous version thereof is the one Faddeev equation for the 3N bound state[10], which is most convenient if one includes a 3NF. For the scattering process this integral equation incorporates all boundary conditions. Using the analytically known form for the free 3N propagator G_0 one obtains[11] the transition amplitude into the 3N breakup configuration as

$$\begin{aligned} f_0 &\equiv \langle \phi_{\vec{p}\vec{q}} \mid tP \mid \psi \rangle \quad (60) \\ &+ \langle \phi_{\vec{p}\vec{q}} \mid (1 + t\ G_0) V_4^{(1)}(1+P) \mid \psi \rangle \\ &\equiv \langle \phi_{\vec{p}\vec{q}} \mid T \mid \phi_{\vec{q}_0} \rangle \quad (61) \end{aligned}$$

Here and henceforth we shall drop the index 1 and refer always to this particular choice of the two-nucleon subsystem, (23). Using Eq.(59) in the definition for T leads immediately to the central Faddeev-like integral equation[12] for $T \mid \phi\rangle$:

$$\begin{aligned} T \mid \phi \rangle &= tP \mid \phi \rangle + (1 + t\ G_0) V_4^{(1)}(1+P) \mid \phi \rangle \quad (62) \\ &+ tP\ G_0 T \mid \phi \rangle + (1 + t\ G_0) V_4^{(1)}(1+P) G_0\ T \mid \phi \rangle \end{aligned}$$

This form underlies our numerical treatment. According to Eq.(53) the full breakup amplitude is given by

$$\langle \phi_{\vec{p}\vec{q}} \mid U_0 \mid \phi_{\vec{q}_0} \rangle = \langle \phi_{\vec{p}\vec{q}} \mid (1+P) T \mid \phi_{\vec{q}_0} \rangle \quad (63)$$

We refer to Ref. 12 for the algebraic steps verifying that the form given in Eq.(63) is identical to the one given in Eq.(41).

It is illustrative to iterate Eq.(62) and thus generate the part of the multiple scattering series for the break-up process which ends with one and the same last t-operator. (In our notation acting between nucleons 2 and 3). The remaining two other pieces for U_0 are given by $PT \mid \phi\rangle$ according to Eq.(63).

Eq.(59) also provides the asymptotic behaviour in the deuteron channel. To see this one rewrites $G_0 t_1$ into $G_1 V_1$ and notes that $(1 + G_0 t_1) G_0 = G_1$. Here G_1 is the channel resolvent operator $(E + i\epsilon - H_1)^{-1}$. Using the analytically known form of G_1 in the deuteron channel[11] one extracts the elastic amplitude as

$$\begin{aligned} f &= \langle \phi' \mid VP \mid \psi \rangle + \langle \phi' \mid V_4^{(1)}(1+P) \mid \psi \rangle \\ &= \langle \phi' \mid VP \mid \{ \mid \phi \rangle + G_0 T \mid \phi \rangle \} + \quad (64) \\ &+ \langle \phi' \mid V_4^{(1)}(1+P) \{ \mid \phi \rangle + G_0 T \mid \phi \rangle \} \end{aligned}$$

The second equality results from Eqs.(59) and (61). Using Eq.(56) one arrives at the more concise form

$$f \equiv \langle \phi' \mid U \mid \phi \rangle \quad (65)$$

with the operator for elastic scattering given as

$$U = PG_0^{-1} + PT + V_4^{(1)}(1+P)(1 + G_0\ T). \quad (66)$$

Again the connection to the standard form is laid out in Ref. 12. Eq.(63) for the break-up amplitude and Eqs. (65) and (66) for the elastic amplitude are central to our numerical treatment.

0.1.4. Connection to the Triad of Lippmann Schwinger Equations

It has been known for a long time[13] that the Lippmann Schwinger (L.S.) equations for more than 2 particles in general do not define scattering states uniquely. However, supplemented by suitably chosen additional L.S. equations one can form a set of equations, which defines the various scattering states uniquely. This was formulated for the 3-body system in Ref. 8 and later was generalized to N particles[14]. Since L.S. equations allow simple access

to the various asymptotic behaviours of 3-body scattering states and in addition a very simple approach to Faddeev equations of various types, we briefly display this formalism. The scattering state $\mid \Psi_{\vec{q}}^{(+)}\rangle_1$ introduced in Eq.(13) obeys the L.S. equation

$$\mid \Psi_{\vec{q}}^{(+)}\rangle_1 = \phi_1 + G_1(V_2 + V_3 + V_4) \mid \Psi_{\vec{q}}^{(+)}\rangle_1 \tag{67}$$

This follows from the identity

$$G = G_1 + G_1(V_2 + V_3 + V_4)G \tag{68}$$

for the full resolvent operator

$$G \equiv (E + i\epsilon - H)^{-1}. \tag{69}$$

If, however, we relate G to G_2 or G_3 we encounter relations

$$\lim_{\epsilon \to 0} \; i\epsilon \; G_{2,3} \; \phi_1 = 0 \tag{70}$$

known as Lippmann identities[15]. The simple arguments for the validity of Eq.(70) can be found in Ref. 7. More rigorous investigations are given in Ref. 16.

As a consequence of Eq.(70) the stationary scattering state $\mid \Psi_{\vec{q}}^{(+)}\rangle_1$ also obeys the two homogeneous equations

$$\mid \Psi_{\vec{q}}^{(+)}\rangle_1 \;=\; G_2(V_3 + V_1 + V_4) \mid \Psi_{\vec{q}}^{(+)}\rangle_1 \tag{71}$$

$$\mid \Psi_{\vec{q}}^{(+)}\rangle_1 \;=\; G_3(V_1 + V_2 + V_4) \mid \Psi_{\vec{q}}^{(+)}\rangle_1 \tag{72}$$

Without V_4 this set of equations has been shown[8] to uniquely define $\mid \Psi_{\vec{q}}^{(+)}\rangle_1$. The proof remains valid if V_4 is present. The argument for a 3N system is simply the following. Besides $\mid \Psi_{\vec{q}}^{(+)}\rangle_1$ there are two more scattering states $\mid \Psi_{\vec{q}}^{(+)}\rangle_2$ and $\mid \Psi_{\vec{q}}^{(+)}\rangle_3$, which are also initiated in a nucleon-deuteron configuration. As $\mid \Psi_{\vec{q}}^{(+)}\rangle_1$ obeys Eqs.(71) and (72) so do $\mid \Psi_{\vec{q}}^{(+)}\rangle_2$ and $\mid \Psi_{\vec{q}}^{(+)}\rangle_3$ obey the homogeneous equation related to Eq.(67). Therefore, Eq.(67) by itself allows an arbitrary admixture of $\mid \Psi_{\vec{q}}^{(+)}\rangle_2$ and $\mid \Psi_{\vec{q}}^{(+)}\rangle_3$ on top of $\mid \Psi_{\vec{q}}^{(+)}\rangle_1$. If we require in addition $\mid \Psi_{\vec{q}}^{(+)}\rangle_1$ to obey Eq.(71), then the admixture of $\mid \Psi_{\vec{q}}^{(+)}\rangle_2$ is excluded and likewise Eq.(72) excludes the admixture of $\mid \Psi_{\vec{q}}^{(+)}\rangle_3$. Since every solution of the triad given in Eqs.(24) - (26) is a solution of the 3N Schödinger equation to the energy E, it remains to verify that the only remaining scattering states initiated by three free nucleons do not obey this set of three equations. Such a state - there is an infinity of them due to the arbitrary choice how the total energy E is distributed over the two relative motions - is defined by

$$\Psi_{\vec{p}\vec{q}}^{(+)} = \lim_{\epsilon \to 0} \; i\epsilon \; G \; \phi_{\vec{p}\vec{q}} \tag{73}$$

Using again the resolvent identities of the type given in Eq.(68) one can easily show[7] that $\Psi_{\vec{p}\vec{q}}^{(+)}$ obeys inhomogeneous equations with the driving terms $\phi_{\vec{p}\vec{q}}^{(+)} \equiv \mid \vec{p}\rangle^{(+)} \mid \vec{q}\rangle$. Here $\mid \vec{p}\rangle^{(+)}$ is a two-nucleon scattering state. Thus the set of Eqs.(67), (71) and (72) is necessary and sufficient to define $\mid \Psi_{\vec{q}}^{(+)}\rangle_1$ uniquely.

The transition amplitudes from the initial channel with particle 1 as projectile to the two-body fragmentation with the single nucleon i can be read off immediately from the proper equation in that set as

$$\langle \phi_i \mid U_{i1} \mid \phi_1\rangle \equiv \langle \phi_i \mid V_j + V_k + V_4 \mid \Psi_{\vec{q}}^{(+)}\rangle_1 \tag{74}$$

Now we split the 3NF V_4 into three parts as given in Eq.(49). This leads to

$$U_{i1} \mid \phi_1\rangle = (\tilde{V}_j + \tilde{V}_k + V_4^{(i)}) \mid \Psi_{\vec{q}}^{(+)}\rangle_1 \tag{75}$$

with the definition

$$\tilde{V}_l \equiv V_l + V_4^{(l)}. \tag{76}$$

Then we use the triad such that $\tilde{V}_l$ and $V_4^{(i)}$ act on the equations with the resolvent operator G_l and G_i, respectively. It follows that

$$\begin{aligned} U_{i1} \mid \phi_1\rangle &= V_4^{(1)} \mid \phi_1\rangle + \bar{\delta}_{i1} \; V_1 \mid \phi_1\rangle \\ &+ \sum_{k \neq i} \tilde{V}_k \; G_k \; U_{k1} \mid \phi_1\rangle + V_4^{(i)} G_i U_{i1} \mid \phi_1\rangle, \end{aligned} \tag{77}$$

or for any of the three possible two-body fragmentations in the initial state

$$\begin{aligned} U_{ij} \mid \phi_j\rangle &= V_4^{(j)} \mid \phi_j\rangle + \bar{\delta}_{ij} V_j \mid \phi_j\rangle \\ &+ \sum_{k \neq i} \tilde{V}_k \; G_k \; U_{kj} \mid \phi_j\rangle + V_4^{(i)} G_i U_{ij} \mid \phi_j\rangle \end{aligned} \tag{78}$$

Here we used the symbol $\bar{\delta}_{ij} \equiv 1 - \delta_{ij}$. In the driving term of Eq.(78) one can replace $V_j \phi_j$ by $G_0^{-1} \phi_j$. Without the 3NF contribution this set is known as the Alt-Grassberger-Sandhas (AGS) equations[17].

According to Eqs.(19) and (75) the fully antisymmetrized transition amplitudes into a two-body fragmentation with single nucleon i are given by

$$U_i \mid \phi\rangle_1 \;\equiv\; \sum_j U_{ij} \mid \phi_j\rangle \tag{79}$$

$$\;=\; (\tilde{V}_j + \tilde{V}_k + V_4^{(i)}) \mid \Psi_{\vec{q}}^{(+)}\rangle_a \tag{80}$$

It follows that the three amplitudes $U_i \mid \phi\rangle_1, i = 1, 2, 3$ have the same functional form, and one has

$$U_2 \mid \phi\rangle_1 \;=\; P_{12}P_{23} \; U_1 \mid \phi_1\rangle \tag{81}$$

$$U_3 \mid \phi\rangle_1 \;=\; P_{13}P_{23} \; U_1 \mid \phi_1\rangle \tag{82}$$

Furthermore, using the three sets of coupled equations given in Eq.(78) and the definition in Eq.(79) one obtains immediately

$$\begin{aligned} U_1 \mid \phi\rangle_1 &= \sum_j V_4^{(j)} \mid \phi_j\rangle + \sum_j \bar{\delta}_{ij} V_j \mid \phi_j\rangle \\ &+ \sum_{k\neq i} \tilde{V}_k \; G_k \; U_k \mid \phi\rangle_1 + V_4^{(i)} G_i U_i \mid \phi\rangle_1 \end{aligned} \tag{83}$$

With the help of Eqs.(17),(76), (81), (82), and (58) setting $U_1 \equiv U$, one obtains the operator relation

$$\begin{aligned} U &= (1+P)V_4^{(1)} + P\; G_0^{-1} \\ &+ (1+P)V_4^{(1)} \; G_1 \; U + Pt \; G_0 \; U \end{aligned} \tag{84}$$

This form of the Faddeev equation without 3NF is the standard starting point, when t-operators of finite rank are used[18]. For general t-operators they are not convenient[9] and it is advisable to separate the right hand side of Eq.(84) into two parts, one without and with P to the left:

$$\begin{aligned} U \equiv \quad & V_4^{(1)} + V_4^{(1)} \; G_0(1+tG_0)U + PG_0^{-1} \\ & + PT \end{aligned} \tag{85}$$

where

$$T = V_4^{(1)} + V_4^{(1)} \; G_0(1+tG_0)U + tG_0 \; U \tag{86}$$

The comparison of Eq.(86) and Eq.(84) reveals immediately the relation

$$(1+P)T + P\; G_0^{-1} = (1 + t\; G_0)U \tag{87}$$

Inserting U from Eq.(85) into Eq.(86) and using the relation given in Eq.(87), one finds easily the integral equation for T, which reads

$$\begin{aligned} T = tP &+ tPG_0T + (1+tG_0)V_4^{(1)}(1+P) \\ &+ (1+tG_0)V_4^{(1)}G_0(1+P)T \end{aligned} \tag{88}$$

Furthermore, the relation of Eq.(87) yields, when inserted into Eq.(85),

$$\begin{aligned} U = V_4^{(1)}(1+P) &+ PG_0^{-1} + V_4^{(1)}G_0(1+P)T \\ &+ PT \end{aligned} \tag{89}$$

The two equations, Eq. (88) and Eq. (89) are identical to Eqs.(62) and (66) from Section 0.1.3.

0.1.5. Spin Observables

Besides the cross sections a very rich set of spin observables is the decisive source of information on the spin dependencies of nuclear interactions including 3NF's. As will be exemplified in Section 0.1.8 one can expect that the 3N continuum will play a very important role to determine properties of 3NF's. The natural language for spin observables is the one of density matrices , which takes into account the statistical nature of the spin directions for beam and target particles. We refer to[1,19] for the formulation of the spin states of spin 1/2 and spin 1 particles in terms of cartesian polarization vectors and tensors. Here we briefly outline the formulation[20] in terms of nonhermitian tensor operators

$$\tau_{kq} \quad k = 0, 1, \cdots, 2s; \quad q = -k, -k+1, \cdots, k \tag{90}$$

for particles of arbitrary spin s. They are defined by their matrix elements with respect to standard spin states $\mid s\mu\rangle, \mu = -s, \cdots, s$ as

$$\langle s\mu' \mid \tau_{kq} \mid s\mu\rangle = \sqrt{2s+1}(-1)^{s-\mu} C(ssk, \mu', -\mu, q) \tag{91}$$

In the following these matrices of dimension $(2s+1)\times(2s+1)$ will be also denoted by τ_{kq}. They have the properties

$$Tr(\tau_{kq}\tau^+_{k'q'}) = (2s+1)\delta_{kk'}\delta_{qq'} \tag{92}$$

and

$$\tau^+_{kq} = (-)^q \tau_{k,-q} \tag{93}$$

Their number is apparently $(2s+1)^2$, which is sufficient to expand the hermitian density matrix ϱ for particles of spin s in terms of them:

$$\varrho \equiv \frac{1}{2s+1} \sum_{kq} t_{kq} \tau^+_{kq} \tag{94}$$

As a consequence of Eq.(92) and assuming $Tr(\varrho) = 1$ it follows for the coefficients t_{kq}

$$t_{kq} = Tr(\varrho\tau_{kq}) \equiv \langle \tau_{kq}\rangle \tag{95}$$

The expectation values $\langle\tau_{kq}\rangle$ and consequently the density matrix ϱ can be expressed in terms of the observables[19]. The advantage of working with the set of complex numbers t_{kq} is that they transform simply under rotations, which are often required in the description of polarizations. For a rotation of one coordinate system into another one through Euler angles α, β, γ one obtains

$$t'_{kq} = \sum_{q'} D^{(k)}_{q'q}(\alpha, \beta, \gamma) t_{kq'} \tag{96}$$

The Madison convention[21] recommends coordinate systems, which turn out to be in order to avoid misunderstandings.

We now express the density matrix of the initial spin states for two independent particles in a different way. Using the complete basis of spin states describing two particles with spins s_1 and s_2,

$$\mid \lambda_i\rangle \equiv \{\mid s_1 m_1\rangle, \mid s_2 m_2\rangle\} \tag{97}$$

one can represent any pure spin state $\mid n\rangle$ by

$$\mid n\rangle = \sum_i a_i^n \mid \lambda_i\rangle \tag{98}$$

and the density operator as

$$\hat{\varrho} \equiv \sum_n \mid n\rangle p_n \langle n \mid \tag{99}$$

Here the normalized numbers p_n denote the probabilities to find the pure spin state $\mid n\rangle$ in the mixed state of beam and target particles. Obviously for the density matrix the result is

$$\varrho_{ij} \equiv \langle \lambda_i \mid \hat{\varrho} \mid \lambda_j\rangle = \sum_n a_i^n p_n a_j^{n*} \tag{100}$$

Now let us assume a reaction leading from two incoming particles with spins s_1 and s_2 to a certain number of outgoing particles with spins s_j. This process is described by the transition amplitude $T^{\{s_1 m_1 s_2 m_2\}}_{\{s_j \mu_j \cdots\}}$. The elastic and break-up amplitudes of Eqs.(33) and (41) are examples thereof. Of course they depend in addition on initial and final momenta, and in our case of three nucleons also on the type of nucleons involved. The quantities

$$b^n_{\{s_j \mu_j \cdots\}} \equiv \sum_{\{m_1 m_2\}} T^{\{s_1 m_1 s_2 m_2\}}_{\{s_j \mu_j \cdots\}} \; a^n_{\{s_1 m_1 s_2 m_2\}} \tag{101}$$

describe the coefficients of the various spin states in the final state analogously to $a_i^n \equiv a^n_{\{s_1 m_1 s_2 m_2\}}$ for the initial state (see Eq.(98)). This is obvious from the asymptotic behaviour in Eqs.(48) and (67). Here an overall normalization factor for T is irrelevant since it will cancel out for spin observables as shown below. As a consequence the density matrix for the final state is given analogously to Eqs.(99) as

$$\begin{aligned}
\varrho^{out}_{\{\mu_j \cdots\}\{\mu'_j \cdots\}} &= \sum_n b^n_{\{\mu_j \cdots\}} p_n \; b^{n*}_{\{\mu'_j \cdots\}} \\
&= \sum_{m_1 m_2} \sum_{m'_1 m'_2} T^{\{m_i\}}_{\{\mu_j\}} \sum_n a^n_{\{m_i\}} \\
&\; p_n a^{n*}_{\{m_{i'}\}} T^{\{m_{i'}\}*}_{\{\mu_{j'}\}} \\
&= \sum_{m_1 m_2} \sum_{m'_1 m'_2} T^{\{m_i\}}_{\{\mu_j\}} \; \varrho^{in}_{\{m_i\}\{m'_i\}} \; T^{\{m'_i\}*}_{\{\mu'_j\}}
\end{aligned} \tag{102}$$

The density matrix for the initial state occurring in Eq.(102) has been denoted by ϱ^{in}. Thus we end up in obvious matrix notation with the well known form for the density matrix of the final state expressed in terms of ϱ^{in} and the transition amplitude T:

$$\varrho^{out} = T \; \varrho^{in} \; T^+ \tag{103}$$

As a first example we express the cross section summed over the final spin states in terms of ϱ^{out}. It is given as

$$\begin{aligned}
\sigma &= \sum_n \sum_{\{\mu_j\}} \mid \sum_{\{m_i\}} T^{\{m_i\}}_{\{\mu_j\}} \; a^n_{\{m_i\}} \mid^2 \\
&= \sum_{\{\mu_j\}} \varrho^{out}_{\{\mu_j\}\{\mu_j\}} = Tr(\varrho^{out})
\end{aligned} \tag{104}$$

Note that in this case the transition amplitude has to incorporate the proper kinematical factors, which for spin observables will play no role. A special case thereof is for an unpolarized initial state

$$\varrho^{in} \equiv \frac{1}{(2s_1+1)(2s_2+1)} \cdot 1 \tag{105}$$

Then using Eq.(104) and Eq.(103) one finds

$$\begin{aligned}
\sigma_0 &= \frac{1}{(2s_1+1)(2s_2+1)} \sum_{\{m_i\}\{\mu_j\}} |T^{\{m_i\}}_{\{\mu_j\}}|^2 \\
&= \frac{1}{(2s_1+1)(2s_2+1)} Tr(TT^+)
\end{aligned} \tag{106}$$

Let us now regard examples for spin observables. Assume one particle is polarized in the initial state. Then

$$\varrho^{in} = \frac{1}{(2s_1+1)(2s_2+1)} \sum_{kq} t_{kq} \; \tau^+_{kq}(i) \tag{107}$$

describes the initial density matrix, where particle i is polarized. (The unit matrix for the other particle is not shown). The cross section is given according to Eq.(104) as

$$\sigma = \frac{Tr(TT^+)}{(2s_1+1)(2s_2+1)} \sum_{kq} \frac{t_{kq} Tr(T\tau^{(+)}_{kq}(i)T^+)}{Tr(TT^+)} \tag{108}$$

The factors multiplying the different initial state polarizations t_{kq} contain the dynamical information and define the analyzing powers $T^{(i)}_{kq}$:

$$T^{(i)*}_{kq} \equiv \frac{Tr(T\tau^{(+)}_{kq}(i)T^+)}{Tr(TT^+)} \tag{109}$$

Using Eq.(105) and Eq.(108) the cross section takes the form

$$\sigma = \sigma_0 \sum_{kq} t_{kq} T^{(i)*}_{kq} \tag{110}$$

The analyzing powers $T^{(i)}_{kq}$ are determined by measuring cross sections for different 'polarizations' t_{kq} in such a way, that a closed set of equations results from which the $T^{(i)}_{kq}$ can be obtained algebraically. Apparently the analysing powers do not depend on the overall normalisation of T. This is true for all spinobservables.

Later on in Section 0.1.8 we shall encounter nucleon analyzing powers $A_y(p)$, deuteron vector analyzing powers $A_y(d)$ and deuteron tensor analyzing

powers like T_{20}. For the connection of those spin observables in cartesian notation to the nonhermitian tensor notation see[19,20].

Spin correlation coefficients occur if beam and target particles are polarized. Thus

$$\varrho^{in} = \frac{1}{(2s_1+1)(2s_2+1)} \sum_{k_1 q_1 k_2 q_2} t_{k_1 q_1}\ t_{k_2 q_2}\ \tau^+_{k_1 q_1} \tau^+_{k_2 q_2} \tag{111}$$

where the quantities with indices 1 and 2 refer to particles 1 and 2. The resulting cross section is

$$\sigma = \sigma_0 \sum_{k_1 q_1 k_2 q_2} t_{k_1 q_1}\ t_{k_2 q_2}\ T^*_{k_1 q_1 k_2 q_2} \tag{112}$$

with the spin correlation coefficients given as

$$T^*_{k_1 q_1 k_2 q_2} = \frac{Tr(T \tau^+_{k_1 q_1} \tau^+_{k_2 q_2} T^+)}{Tr(TT^+)} \tag{113}$$

We skip the case where the initial state is polarized and the polarization of the outgoing particle(s) is (are) measured.

Finally we mention polarization transfer coefficients. Here one of the initial particles is polarized and the polarization of one of the outgoing particles is measured. The initial density matrix is given as in Eq.(107), and we call now this polarized particle a. The measurable polarization tensors of one outgoing particle, e.g. particle c, are then given by

$$t^c_{k_c q_c} = \frac{Tr(\varrho^{out} \tau_{k_c q_c})}{Tr(\varrho^{out})} = \frac{\sigma_0}{\sigma} \sum_{k_a q_a} t_{k_a q_a} \frac{Tr(T \tau^+_{k_a q_a} T^+ \tau_{k_c q_c})}{Tr(TT^+)} \tag{114}$$

If the polarization transfer coefficients are defined as

$$t^{k_a q_a}_{k_c q_c} \equiv \frac{Tr(T \tau^+_{k_a q_a} T^+ \tau_{k_c q_c})}{Tr(TT^+)} \tag{115}$$

one obtains

$$\sigma t^c_{k_c q_c} = \sigma_0 \sum_{k_a q_a} t_{k_a q_a} t^{k_a q_a}_{k_c q_c} \tag{116}$$

The term with $k_a q_a = 00$ describes the polarization of particle c resulting from an initially unpolarized state. The experimental determination requires the measurement of cross sections and final polarizations for different sets of $\{t_{k_a q_a}\}$.

0.1.6. Actual Implementation

It was a long way to go to arrive at the present day standards, where precise solutions (in a numerical sense) of the 3N Faddeev equations in the continuum are feasible. First, limited computer resources enforced low rank approximations of the NN t-operator. In addition only a severely truncated number of angular momenta could be taken into account. Also, the moving logarithmic singularities (see below) caused a substantial technical obstacle, which was initially overcome by contour deformations and only later by the use of suitable interpolation schemes allowing for arbitrary NN forces. For information on those developments we refer to[22,17,23,24]. An enormous amount of work should be cited in addition. Some of it can be traced back in[1]. Here we would like to present our way to solve the central Faddeev Eq.(62) for the (partial) break-up operator T. Let us first neglect the 3NF. Then Eq.(62) reduces to

$$T|\phi\rangle = tP|\phi\rangle + tP\ G_0\ T|\phi\rangle \tag{117}$$

In this equation the NN t-operator refers to an arbitrary but fixed two-body subsystem. Let us choose the particles 2 and 3 in agreement with the Jacobi momenta given in Eqs.(44) and (45). The equation is solved in a partial wave representation. We introduce the notation

$$\alpha \equiv (ls)j(\lambda\frac{1}{2})I(jI)\mathcal{J}(t\frac{1}{2})T \tag{118}$$

which describes the coupling of the angular momenta l with the total spin s to the total angular momentum j of the two-nucleon subsystem (23), further the coupling of the angular momentum λ, which is related to $\vec{q}$ with the spin 1/2 of particle 3 to its total angular momentum I, finally the coupling of the two angular momenta j and I to the total conserved 3N angular momentum $\mathcal{J}$. The two-body isospin t is coupled with the isospin 1/2 of the third particle to the total isospin T. This set of discrete quantum numbers together with the magnitudes of the Jacobi momenta p and q lead to a complete description of the space of states for three nucleons. We denote the corresponding basis states by $|pq\alpha\rangle$. They are chosen to be orthonormal and satisfy the completeness relation

$$\sum_\alpha \int_0^\infty dp p^2 \int_0^\infty dq q^2 |pq\alpha\rangle\langle pq\alpha| = 1 \tag{119}$$

The initial channel state

$$|\phi\rangle \equiv |\varphi_d\rangle|\vec{q}_0\rangle \tag{120}$$

is composed of a deuteron state and the momentum eigenstate of the projectile particle. The deuteron state is antisymmetric under the exchange of particles 2 and 3. Since the permutation operator P, given in Eq.(17), is symmetric under exchange of particles 2 and 3 like t, the driving term in Eq.(117) remains antisymmetric in particles 2 and 3. The integral operator in Eq.(117) is also symmetric and consequently T will be antisymmetric in that pair. Consequently only a subset of basis states $|pq\alpha\rangle$ is needed,

which is antisymmetric under exchange of particles 2 and 3. This is guaranteed by requiring

$$(-1)^{l+s+t} = -1 \tag{121}$$

The completeness relation given in Eq.(119) is meant to run only over that subset of states. Let us now project Eq.(117) onto $|pq\alpha\rangle$ and insert the completeness relation Eq.(119) two times into the kernel:

$$\begin{aligned}\langle pq\alpha|T\phi\rangle &= \langle pq\alpha|tP|\phi\rangle \\ &+ \sum\!\!\!\!\!\!\int_{\alpha'} \sum\!\!\!\!\!\!\int_{\alpha''} \langle pq\alpha|t|p'q'\alpha'\rangle\langle p'q'\alpha'|P|p''q''\alpha''\rangle \times \\ &\frac{1}{E+i\epsilon-\frac{p''^2}{m}-\frac{3}{4m}q''^2}\langle p''q''\alpha''|T|\phi\rangle\end{aligned} \tag{122}$$

Here we introduce obvious short hand summation symbols and use the fact that the operator of the kinetic energy, H_0, is diagonal in this representation. The kinetic energy related to the Jacobi momenta has the well known form $p^2/m + 3/4mq^2$. The total c.m. 3N energy E related to the initial state ϕ is given by

$$E = E_d + \frac{3}{4m}q_0^2 \tag{123}$$

where $E_d < 0$ is the deuteron binding energy. Obviously Eq.(122) represents an infinite set of coupled integral equations in two continuous variables. Note that for each conserved total angular momentum $\mathcal{J}$ there is an infinite number of ways j and I can couple to $\mathcal{J}$.

The NN t-operator does not act on the quantum numbers of the 'spectator' nucleon. Therefore corresponding diagonality conditions occur. Since t is defined through a L.S.equation containing the free 3N propagator G_0 the effective two-body subsystem energy is $E - \frac{3}{4m}q^2$ and we obtain

$$\begin{aligned}\langle pq\alpha|t|p'q'\alpha'\rangle &= \frac{\delta(q-q')}{qq'}\ \delta_{\lambda\lambda'}\ \delta_{II'} \\ &\langle p(ls)jt|\tau(E-\frac{3}{4m}q^2)|p'(l's)jt\rangle\delta_{ss'}\delta_{tt'}\delta_{jj'}\end{aligned} \tag{124}$$

In Eq.(124) we took into account that s and t is conserved(which we assume here and which is valid to a high degree of accuracy) and where the NN τ-operator is acting in the two-nucleon space only. As is well known l is not conserved in the states where the tensor force is acting. That partial wave projected τ-matrix can be gained numerically in an easy manner by solving the L.S.equation, which is driven by the NN force and which is correspondingly partial wave projected.

The permutation operator P turns out to be more complicated and has the form

$$\begin{aligned}{}_1\langle p'q'\alpha'|P|pq\alpha\rangle_1 &= {}_1\langle p'q'\alpha'|pq\alpha\rangle_2 \\ &+ {}_1\langle p'q'\alpha'|pq\alpha\rangle_3,\end{aligned} \tag{125}$$

where the index 2, for instance, indicates, that p refers to the subsystem (31) and q to the spectator nucleon 2. Clearly also the discrete quantum numbers α are related to those particles in a similar fashion. The evaluation of the matrix elements on the right hand side of Eq.(125) is a purely geometrical problem and will not be discussed here. For various versions thereof we refer to[7,25,26]. We obtain for Eq.(125)

$$\begin{aligned}&{}_1\langle p'q'\alpha'|P|pq\alpha\rangle_1 \\ &= \int_{-1}^{1} dx \frac{\delta(p'-\pi_1)}{p'^{l'+2}}\frac{\delta(p-\pi_2)}{p^{l+2}}\ G_{\alpha'\alpha}(q'qx)\end{aligned} \tag{126}$$

with

$$\pi_1 = \sqrt{q^2+\frac{1}{4}q'^2+qq'x} \tag{127}$$

$$\pi_2 = \sqrt{q'^2+\frac{1}{4}q^2+qq'x} \tag{128}$$

and where $G_{\alpha'\alpha}$ is composed of Legendre functions, powers of q and q' and geometrical quantities like Clebsch Gordon coefficients, and 6j symbols. Using Eqs.(124) and (126) in Eq.(122) we finally obtain

$$\begin{aligned}\langle pq\alpha|T|\phi\rangle &= \langle pq\alpha|tP|\phi\rangle \\ &+ \sum_{\alpha'}\sum_{\alpha''}\int_0^\infty dq'q'^2\int_{-1}^{1}dx \\ &\langle p(ls)jt|\tau(E-\frac{3}{4m}q^2)|\pi_1(l's)jt\rangle \times \\ &\delta_{\bar\alpha\bar\alpha'}\frac{1}{\pi_1^{l'}\pi_2^{l''}}\ G_{\alpha'\alpha''}(q,q'x)\frac{1}{E+i\epsilon-\frac{q^2+q'^2+qq'x}{m}} \times \\ &\langle \pi_2 q'\alpha''|T|\phi\rangle\end{aligned} \tag{129}$$

The Kronecker symbol $\delta_{\bar\alpha\bar\alpha'}$ means $\delta_{\alpha\alpha'}$ with the exception of l and l'. A glance at this set reveals two immediate obstacles. The first argument π_2 of the unknown amplitude under the integral requires interpolation[26,27], since all the π_2-values can not be kept in a discretized grid. This can conveniently and efficiently be achieved by different types of spline interpolations. The same interpolations can be applied to the argument π_1 in the NN τ-matrix. The second, more serious problem are the moving singularities occurring in the free propagator. They occur at locations

$$x = x_0 \equiv \frac{mE-q^2-q'^2}{qq'} \tag{130}$$

If $|x_0| \leq 1$ they appear as Cauchy type singularities in the x-integral. We solve this problem by the method of "subtraction". This leads to two terms, one of which is no longer singular and another one, where the x-integral can be carried through analytically leading to logarithmic singularities in the momenta q and q'. Their positions are given by$|x_0| = 1$.

Those singularities in q' move with the value q chosen on the left. We handle this problem by expanding the accompanying function in q' into splines based on a grid in the q-variable. The deuteron pole in the ${}^3S_1 - {}^3D_1$ τ-matrix is again treated by subtraction. The inhomogeneous term in Eq.(129) requires only interpolations and quadratures.

We end up with an algebraic set of inhomogenous integral equations, whose dimension is given by the product of grid points in p and q and the number of discrete quantum numbers α. Fortunately with respect to the latter, the short range nature of the NN force helps. For energies E up to the pion threshold two-nucleon states up to a maximal value $j = 6$ are sufficient to obtain a converged result. For lower energies around 20 MeV for instance fewer values of j are needed. Thus the infinite set of equations can be truncated to a finite one. Nevertheless one typically needs 200 α-states for each total $\mathcal{J}$. The total $\mathcal{J}$ can be as large as 25/2 for higher energies.Because of the huge dimension of the discretized kernel it is mandatory to use an iterative method to solve this coupled set of equations. By iteration one generates directly the multiple scattering series, a power series in the NN-t-operator, which is present in the driving term and the kernel. The series diverges for the quantum numbers of the 3N bound state $\mathcal{J}^\pi = 1/2^+$ and converges only very slowly for many of the smaller $\mathcal{J}$-values. All those Neumann series are summed up by the Padé technique, which is very efficient and perfectly reliable. Typically 10-20 iterations are required for the smaller $\mathcal{J}$-values. Needless to say this requires powerful computers. Once the amplitudes $\langle pq\alpha|T|\phi\rangle$ are known, the transition amplitudes of elastic nd scattering and the nd break up process can be evaluated by quadratures according to Eqs.(63), (65) and (66).

If one includes 3NF's further terms occur in the central equation given in Eq.(62) and the technical challenge increases dramatically. In a partial wave representation the matrices $\langle pq\alpha|V_4^{(1)}|p'q'\alpha'\rangle$ for each total angular momentum $\mathcal{J}$ and total parity are of very high dimension and require extreme storage resources. Moreover each matrix element requires angular integrations[28]. This is immediately obvious for instance in the case of the 2π-exchange, since the two pion momenta are linear combinations of the Jacobi momenta for initial and final states. This introduces various angles, which have to be integrated to arrive at specific angular momentum states. Therefore after first attemps [28], a more efficient way to evaluate the 3NF matrices had to be introduced[26], which has been realized up to now in the case of the 2π exchange, shown in Fig. 1.

The first diagram in Fig. 1, $V_4^{(1)}$ in our notation,

Figure 1 The 2π-exchange 3N force. The blob indicates the πN (off-shell) amplitude without the nucleon propagation. The first diagram where nucleon 1 is singled out is $V_4^{(1)}$.

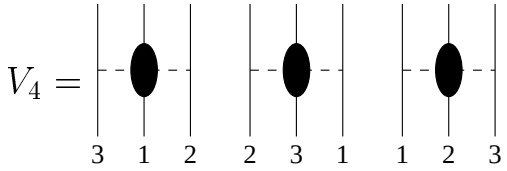

can be evaluated in the following fashion. For the pion exchange between nucleons 1 and 3 one uses the Jacobi momenta such that the pair (13) forms the two-body subsystem and a corresponding other set of Jacobi momenta is used for the pion exchange between nucleons 1 and 2. The central blob in Fig. 1 is in the most simple case just a constant. Thus at that point a recoupling of the two types of Jacobi momenta occurs. This has basically the same form as the matrix element of the permutation operator P. The blob contains in addition momentum- and spin-dependent quantities, which can be separated into two parts and be combined and handled together with the left or the right pion propagators. In that sense the action of $V_4^{(1)}$ is like a sequence of "pair forces" between different pairs, now with no free 3N propagator in between, but essentially only a recoupling process. This way of treating $V_4^{(1)}$ turns out to be very efficient. It is also the only way which allowed us to evaluate $V_4^{(1)}$ for all angular momenta needed for a full convergence. For this task massive parallel supercomputers are extremely helpful if not mandatory.

Finally we would like to mention that the charge-independence and charge- symmetry breaking of the NN forces lead to admixtures of total isospin T=3/2 in addition to the dominant T=1/2 states[29]. For certain scattering observables it is sufficient to keep only T=1/2 but one has to use certain linear combinations of np and nn(pp) t-matrices as prescribed by Clebsch-Gordon coefficients. For other observables, like specific configurations in the nd break-up process T=3/2 admixtures are mandatory[1].

0.1.7. Dynamical Input for Three-Nucleon Calculations

The goal of exact 3N scattering calculations and their comparison with experiment is the test of assumptions about the underlying nuclear Hamiltonian. The strategy is to use the best NN potentials currently available, which describe the NN data up to the pion threshold with highest possible accuracy, and to determine their predictions for observables in a 3N context. Discrepancies between those predictions and

3N data are candidates for 3NF effects. Of course this may be a time-dependent result, since possible future NN forces with different physical ingredients (especially with dynamical nonlocalities at short distances) may change predictions of 3N observables given by NN forces only. One further candidate for an explanation of possible discrepancies are relativistic effects. Estimates for relativistic effects for 3N bound states[30,31] exist, which however have not yet settled and right now there is no general agreement how to control that difficult issue of relativity in few-nucleon systems[32].

One should also mention the formal insight[33] that a 3N Hamiltonian composed of NN and 3NF's can be transformed into another one without 3NF's such that neither the 3N binding energy nor the 3N S-matrix change. Another important consequence of such a transformation is that the NN forces remain phase equivalent. However, here we take the point of view that there is some physical framework underlying the construction of NN and 3N forces, which makes a definite choice among the unitarily equivalent representations.

Theoretical attempts to construct NN forces have a long history. Yukawa initiated the idea of meson-exchange, which found a successful and generalized realization in the form of the one-boson-exchange[34]. In this picture the isovector pseudoscalar pion, an effective isoscalar scalar σ-meson, the isoscalar vector meson ω and the isovector vector meson ρ give the dominant contributions. Of course, the one-boson exchange picture has been successfully extended to include multi-meson exchanges. Parallel to this development several phenomenological forms for NN potentials have been proposed. In recent years a few potentials have been created, which are fitted to the individual partial wave NN phase shift parameters or directly to the NN data base, at the price of a large number of parameters (of the order 40). These are the interactions Nijm II and I[35], the first one being purely local, the second one having weak nonlocalities in the form of $\bigtriangledown^2$ operators, the AV18 potential [36] again weakly nonlocal and the CD Bonn potential[37], which is closest to a meson exchange picture leading to more pronounced nonlocalities. All the latter potentials take into account charge independence and charge symmetry breaking and were at the time of their publication of highest quality with a χ^2 per data point very close to 1. We refer the reader to the original articles for more information. The meson exchange picture based on standard Lagrangians has been pushed beyond the one-boson exchange for instance in the form of the so called full Bonn potential[38], which is energy dependent due to its derivation within the framework of time-ordered perturbation theory. This energy dependence makes it less suitable for use in a system of more than 2 nucleons, since one has to integrate over that two-body subsystem energy, which enters as a parameter into the potential and runs from the actual total energy towards minus infinity. One expects that in such a formulation many- nucleon forces are stronger than in a formulation with energy independent NN forces[39]. In addition, this force has not yet been tuned perfectly well to the NN data set. More modern developments in the context of chiral perturbation theory have also not yet been pushed to that degree of accuracy in describing NN data[40] that their use in 3N scattering would be justified except for qualitative insights. However, one can expect very important theoretical guidances[41] in constructing nuclear forces (including 3NF's) since for the first time in nuclear physics one has a smallness parameter in the low momentum region where chiral perturbation theory is valid.

With respect to 3NF's the present status is in an even earlier development stage than in the case of NN forces. The old idea of Fujita-Miyazawa[42] is still very alive. This model generates a 3NF by the process that one nucleon emits a pion, which is absorbed by a second one and which then turns into a Δ isobar. This intermediate Δ deexcites again into a nucleon emitting a second pion, which is then absorbed by the third nucleon. Since in the intermediate state one has two nucleons and a Δ one leaves the 3N Hilbert space and consequently the process can not be represented as a sequence of pion exchanges between different pairs of nucleons. It is a 3NF. This model has been refined[43] by replacing the intermediate Δ by the fully off-the-mass-shell πN scattering amplitude (with the forward propagating nucleon piece subtracted). This amplitude is described theoretically in a low momentum expansion. Several versions thereof exist[44,45] in the literature. In addition extensions to $\pi - \rho$ and $\rho - \rho$ exchanges have been proposed[46]. Chiral perturbation theory can be expected to bring some order into the large number of possible 3NF diagrams[47]. Another often used 3NF model originated from the Urbana-Argonne group[48]. This model incorporates 2π-exchanges at larger distances and a phenomenological short range structure. Last not least one should mention the Ruhr Pot model[49], which so far has not yet been applied in 3N studies.

Our numerical results to be presented in Section 0.1.8 are based on the following temporary strategy. It is well established by several groups that ^{3}He and ^{3}H is not correctly bound by the present day NN forces. We show in Table 1 our fully converged Faddeev results for the four presently most accurate NN potentials. In case of ^{3}He we also in-

Table 1 Theoretical binding energies for ^{3}He and ^{3}H based on modern NN forces. We see underbinding with respect to the experimental values.

Potential	B(^{3}He) [MeV]	B(^{3}H) [MeV]
CD-Bonn	-7.29	-8.01
Nijm I	-7.09	-7.74
Nijm II	-7.01	-7.65
AV18	-6.96	-7.67
Experiment	-7.72	-8.48

clude the Coulomb force and we always take charge independence and charge symmetry breaking into account. We see some spread of the theoretical predictions with the CD Bonn results being closest to the experimental values, but in all cases a clear underbinding. In relation to those NN forces additional dynamics is needed, which most likely will be the action of 3NF's. We have chosen the 2π-exchange Tucson-Melbourne 3NF model (TMF)[43] as the "vehicle" to provide some first insights of possible 3NF effects. Naturally other force models will follow and we can expect a very exciting search[41] in establishing the strength and properties of 3NF's. A phenomenological way is to adjust one parameter in that TMF such that together with a chosen NN force the correct 3N binding energy results. For this parameter we have chosen the cut-off value Λ of the strong form factor entering into that force model. Since the interplay of the four NN forces with the TMF model depends on the choice of the force (in other words NN forces and 3NFs are not consistent from a theoretical point of view), one has to expect that this crude approach leads to cut-off parameters Λ, which depend on the NN force. This is indeed the case[50]. For the standard monopole form factors employed in this model the cut-off values Λ range between 4.8 m_π and 5.2 m_π; the smallest one is needed for CD Bonn because of its smallest underbinding. In such a manner we arrive at four 3N Hamiltonians including the properly adjusted TMF, which by construction give the correct 3N binding energy.

Finally we mention the approach to extend the Hilbert space and to allow for the occurrence of one Δ (or more) in the 3-body wavefunction. In such a manner 3NF effects generated by the Δ-degree of freedom are incorporated as transition potentials. For the 3N bound state the most advanced calculation have been performed in [77]. For the 3N scattering only one Δ-admixture has been allowed so far. Though this picture[51] appears quite promising, right now the fine tuning to NN data is still missing and therefore predictions in the 3N sector suffer somewhat from that uncertainty.

0.1.8. Comparison of Theory and Experiments in Three-Nucleon Scattering

We use today's most modern NN forces and solve the Faddeev equations exactly (in a numerical sense). There are no free parameters. Let us first consider the NN force only predictions. The most simple (fully integrated) observable is the total nd cross section[52], which is shown in Fig. 2. The calculation is based on the CD BONN potential, however the other NN forces (AV18, Nijm I and II) will give identical results[53] (within about 1%). This statement is also valid for all cross sections shown in this section, similarily for many spin observables. In such a case of stability of the NN force predictions, discrepancies to data can possibly be considered to be signatures of 3NF's. However there are some spin-observables, where different NN force predictions show a spread which is comparable in size to the one introduced by adding a 3NF. Here we show only predictions from CD Bonn and refer for results for other potentials to the original literature, especially to Ref. [1]. In Fig.2 we see a perfect agreement with experiment at low energies, but a tendency towards a slight underprediction of the data near 100 MeV ($\approx$4%).

Next we consider the angular distributions of the differential cross section in elastic Nd scattering. We are not yet able to include the pp Coulomb force into our rigorous calculations. Therefore all our predictions are for the nd system.Nevertheless we compare to pd data, since they are more numerous and have smaller error bars. There are first attemps in the literature to include the pp Coulomb force[54] above the deuteron break-up threshold, however those are still based on an approximate treatment of the strong force. Thus those results are not yet definite enough to allow for a reliable estimate of Coulomb force effects. For energies below the break-up threshold variational techniques formulated in configuration space and based on hyperspherical harmonic expansions have mastered the pp Coulomb problem. We refer the reader to[65]. We show in Figs. 3-5 differential cross sections at three more or less arbitrarily selected energies. At the two lower energies the agreement is perfect except at the very forward angles, where Rutherford scattering is obviously present, and which is not included in our theory. At 65 MeV in the minimum there is a clear underestimation of the data by the theoretical prediction, which as we shall argue below, is very likely a signature of 3NF effects.

The first spin observable we consider next is the nucleon analyzing power A_y in elastic nd scattering. Figs. 6 and 7 show theory with respect to the data

Figure 2 The calculated total nd cross section (solid line) together with the experiment[52].

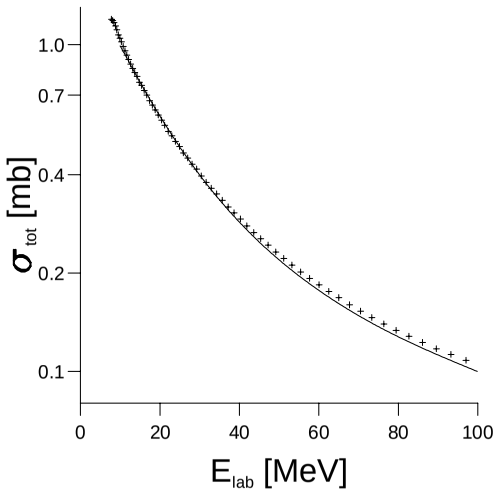

Figure 3 The calculated angular distribution of the differential cross section for elastic nd scattering plotted against pd data [55] at $E_{lab} =$ 12 MeV.

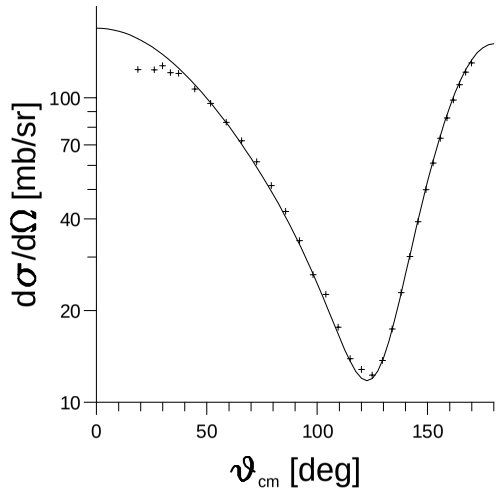

at $E_{lab} = 3$ and 10 MeV. We see a strong underprediction of the theory with respect to the data, which is often called the low-energy A_y-puzzle[66]. This observable is very sensitive to the ^3P_j NN force components. This suggests that a possible reason for the discrepancy could result from a not yet sufficiently well settled phase-shift analysis for the ^3P_j states[67]. If this conjecture turns out to be incorrect, one very likely sees a strong signature of 3N force effects[68].

Figure 4 The same as in Fig. 3 for $E_{lab} = 22.7MeV$

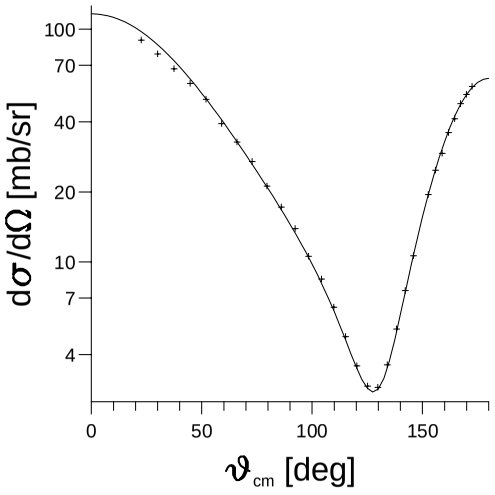

Figure 5 The same as in Fig.3, now at $E_{lab} = 65MeV$ and with pd data from [56]

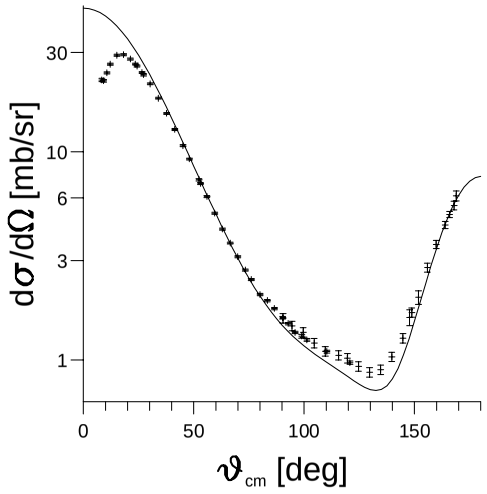

At higher energies, starting around 30 MeV, this discrepancy is no longer present, see Figs. 8 and 9

The tensor analyzing powers seem to be very well predicted by NN forces only as exemplified in Fig. 10 for T_{20}. These are again pd data compared with nd calculations, and the last word to be spoken has to wait until Coulomb force effects have been rigorously taken into account.

As a last example for spin observables in elastic scattering we show the spin transfer coefficient $K_y^{y'}$ at 19 MeV in Fig. 11. There is a small discrepancy

Figure 6 The analyzing power A_y[57] for elastic nd scattering at $E_{lab} = 3$MeV plotted against theory

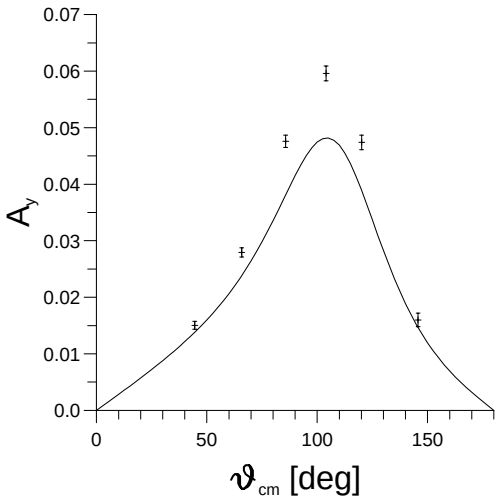

Figure 8 The same as in Fig. 6, now at $E_{lab} = 30MeV$ and with nd data from [59].

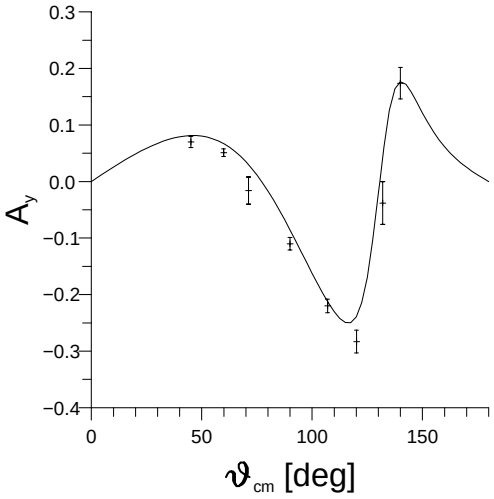

Figure 7 The same as in Fig. 6, now at $E_{lab} = 10MeV$ and with nd data from [58]

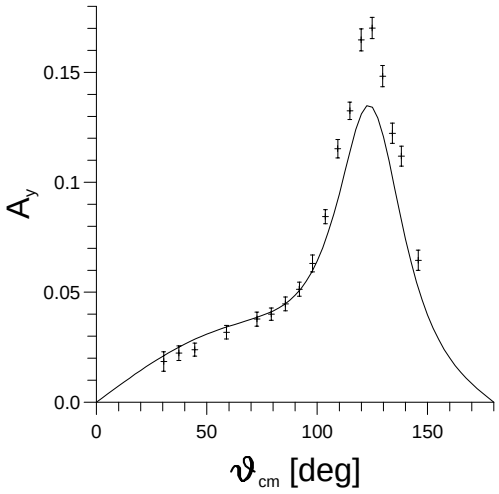

Figure 9 The same as in Fig. 6, now at $E_{lab} = 65MeV$ and with pd data from [56].

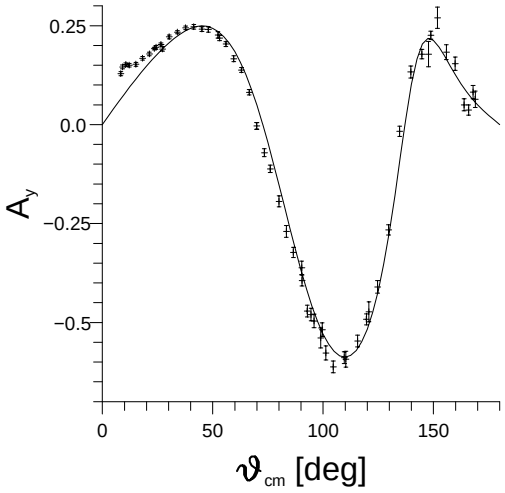

in the minimum, which might be caused by Coulomb force and/ or 3NF effects (see below).

There are many more examples for spin observables in nd elastic scattering and we refer to the review article[1] for further cases.

In the break-up process there is a continuum of observables and up to now only special break-up configurations have been selected according to some "prejudices". We show a few and refer again to[1] for more information. We always display the five-fold differential cross section from Eq.(46) as a function of the arclength S on the kinematically allowed locus. The quasi free scattering condition (where one of the three nucleon laboratory momenta is zero) has often been investigated in the past. The simple idea here is that one of the nucleons is a spectator. In a plane wave impulse approximation one can see directly[1] that this condition leads to a zero argument of the deuteron wavefunction and thus to a peak. In reality at least below about 100 MeV this picture is

Figure 10 The tensor analyzing power T_{20} [55] for elastic pd scattering at $E_{lab} = 22.7MeV$ against theory.

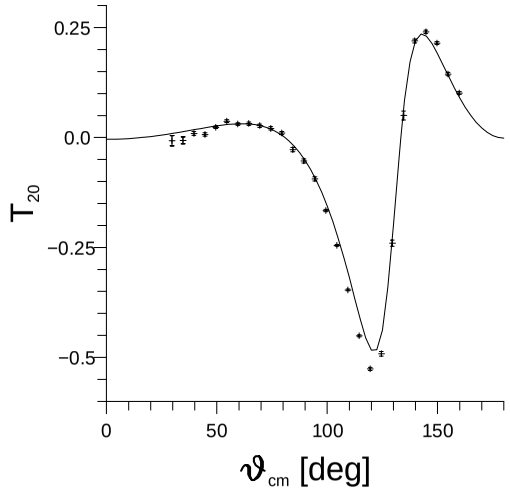

Figure 11 The spin transfer coefficient $K_y^{y'}$ for elastic pd scattering [60] at $E_{lab} = 19MeV$ plotted against theory

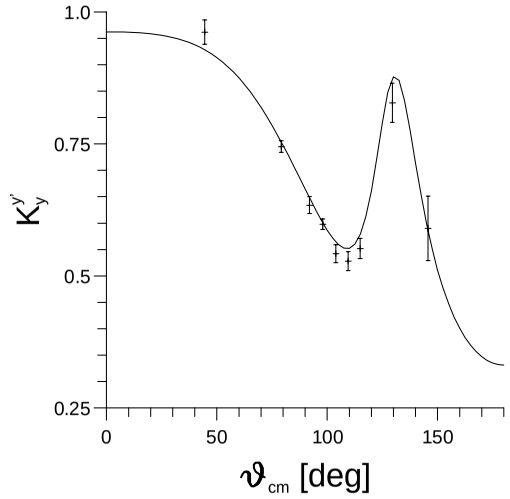

completely unjustified, since the rescattering is non-negligible. Nevertheless, the peak structure survives, which is shown in one example in Fig. 12. Again pd data are compared to nd theory, and the agreement is quite good.

Another often studied break-up configuration is the so called FSI condition. In that case two nucleons leave with equal momenta and thus with a relative energy going to zero. This has the obvious

Figure 12 The pd break-up cross section [61] as a function of the arc length S of the kinematical locus for detector angles $\Theta_1 = 44° = \Theta_2$ and $\phi_{12} = 180°$ at $E_{lab} = 65MeV$ plotted against theory.

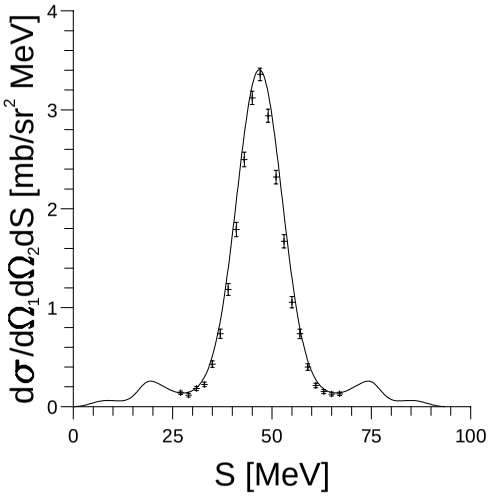

Figure 13 The pd break-up cross section [62] as a function of the arc length S of the kinematical locus for $\Theta_1 = 39°, \Theta_2 = 62.5°$ and $\phi_{12} = 180°$ at $E_{lab} = 13MeV$ and compared to theory.

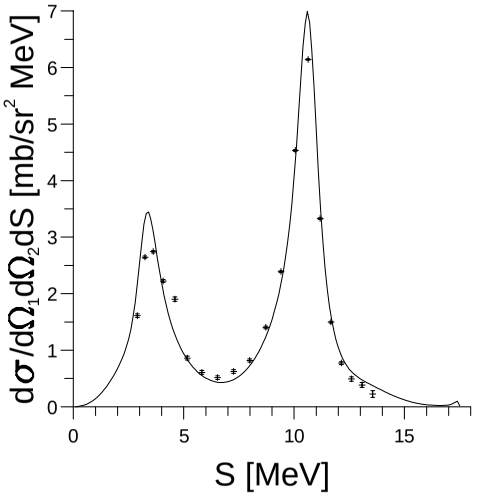

consequence that the NN t-operator is probed at zero two-body subsystem energy, an energy which is close to the pole of t in the state $^1S_0$. This discrete two-body state is often denoted as virtual state. The nearby pole causes the strong enhancement seen in Fig. 13 for specific S-values. The theoretical calculation is carried out for point geometry (vanishing open angles of the two detectors and sharp energy

Figure 14 The pd break-up cross section [62] as a function of the arclength S of the kinematical locus for $\Theta_1 = 50.5° = \Theta_2, \phi_{12} = 120°$ at $E_{lab} = 13MeV$ compared with theory.

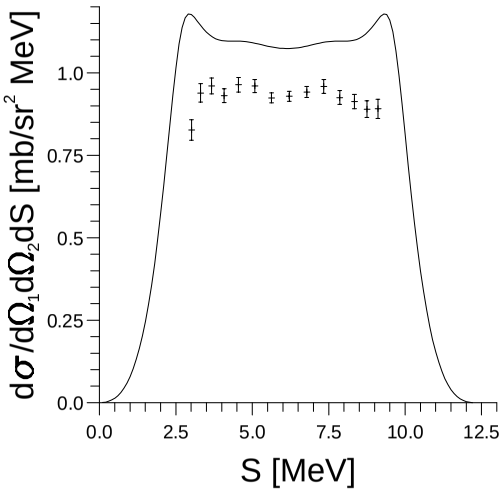

Figure 15 The same as in Fig. 14, now for $\Theta_1 = 52° = \Theta_{12} = 120°$ at $E_{lab} = 19MeV$ [62] against theory.

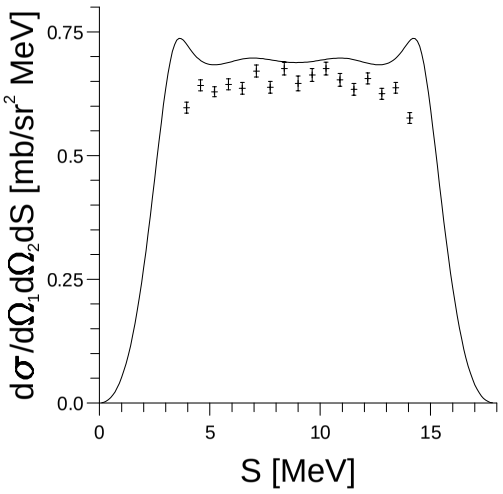

Figure 16 The same as in Fig. 14, now for $\Theta_1 = 54° = \Theta_2, \phi_{12} = 120°$ at $E_{lab} = 56MeV$ [61] against theory.

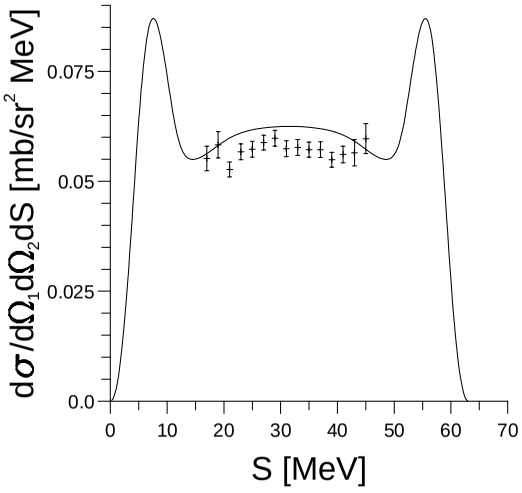

Figure 17 The analyzing power A_y [61] for pd break-up as a function of S for $\Theta_1 = 35.2° = \Theta_2, \phi_{12} = 180°$ at $E_{lab} = 65MeV$ against theory.

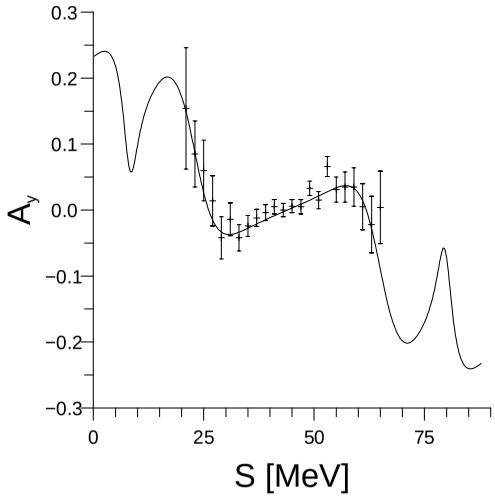

resolution). When the experimental opening angles are taken into account the agreement with the data is very good[62]. Those FSI peaks have been used very often in the past to extract the nn scattering length in the nd break-up process. The results were always very controversial. Only recently a renewed measurement combined with a very elaborated theoretical analysis based on rigorous solutions to the Faddeev equations and on modern NN forces reached a result[69] for the nn scattering length a_{nn}, which agrees rather well with the value found in the $\pi^- d$-capture process. A parallel investigation to extract the well known np scattering length in the state $^1S_0$ also leads to the correct result, which is gratifying and indicates that 3NF effects in that process should be rather weak.

Finally we show in Figs. 14-16 break- up cross sections for the so called space-star configuration, where

Figure 18 The total nd cross section [52] (extension of Fig. 2) against theory.

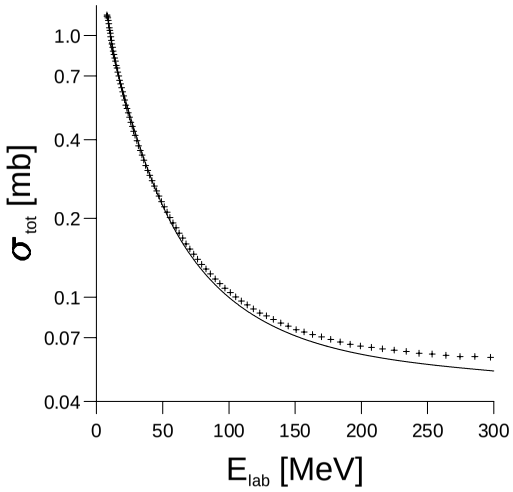

Figure 19 The differential cross section for elastic nd scattering without (solid curve) and with 3NF (dashed curve) at $E_{lab} = 65MeV$. pd data as in Fig. 5

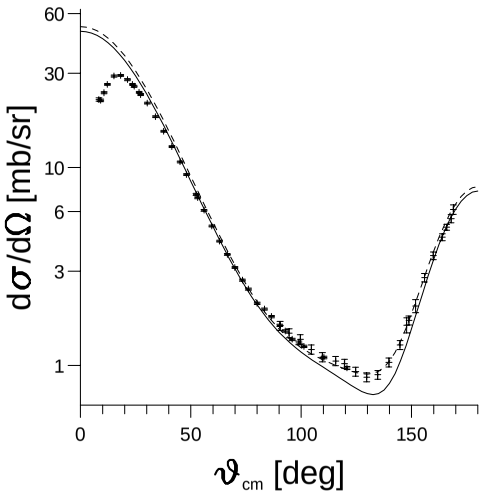

Figure 20 Same as in Fig. 19 at $E_{lab} = 135MeV$ pd data from [63]

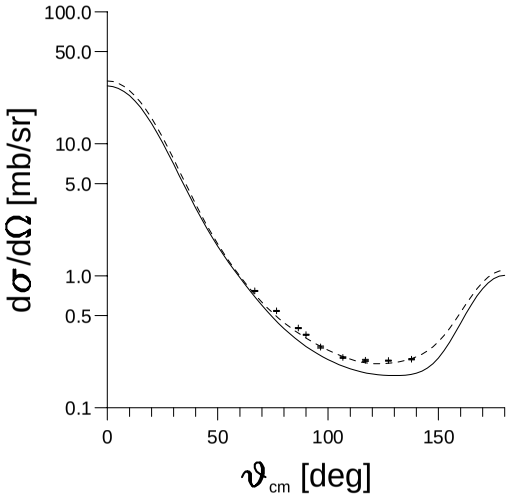

Figure 21 The deuteron vector analyzing power A_y for elastic nd scattering without (solid curve) and with 3NF (dashed curve) at $E_{lab} = 135MeV$. pd data from [63]

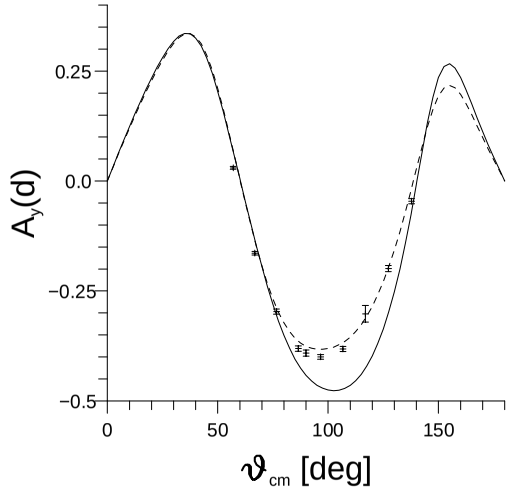

the three nucleons leave with equal momenta in magnitudes and under pairwise angles of 120° in a plane, which is orthogonal to the beam direction in the c.m. system. This very symmetric configuration was in the past considered to be a good candidate to see 3N force effects. We show in the figures pd data for three energies. At the lowest energy theory overpredicts the data, which might be due to the neglection of Coulomb forces. Then at the two higher energies data and theory come closer together. Again only a strict evaluation with Coulomb forces will reveal, whether 3NF effects (deviations from NN force predictions only) will remain.

Spin observables for three-nucleon break-up processes are still rather scarce. We show one example, the proton analyzing power A_y at 65 MeV in Fig. 17. The agreement with experiment is quite good. We expect that spin observables in the break up process

Figure 22 The nucleon analyzing power $A_y(p)$ in elastic nd scattering at a fixed deuteron recoil angle of $\Theta_{lab} = 42.6^\circ$ as a function of energy without (solid curve) and with 3NF (dashed curve).pd data from [64]

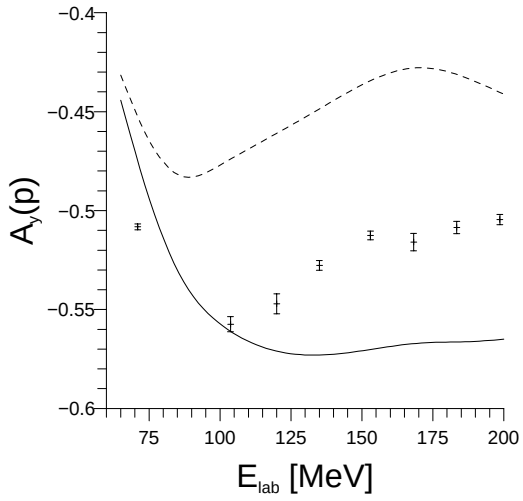

Figure 23 A spin correlation coefficient in elastic nd scattering without (solid curve) and with 3N force (dashed curve) at $E_{lab} = 190 MeV$.

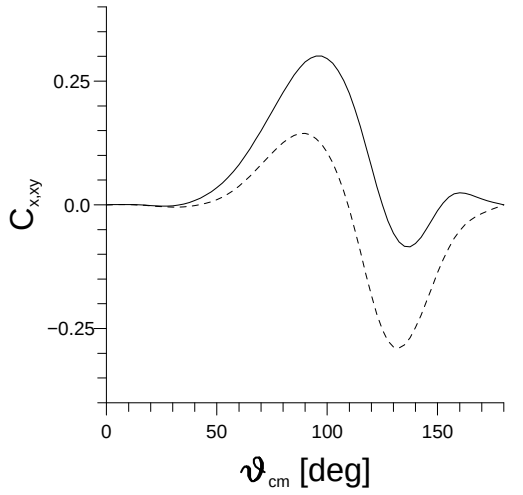

will play an important role in the future to reveal the structure of 3NF's.

We now consider higher energies and our first sufficiently well converged calculations including a 3NF. The results will be based on the TMF model, which has been adjusted to the 3N binding energy as described in Section 0.1.7. We begin with the total nd cross section extended now up to about 300 MeV in

Figure 24 Same as in Fig. 23 for a spin transfer coefficient.

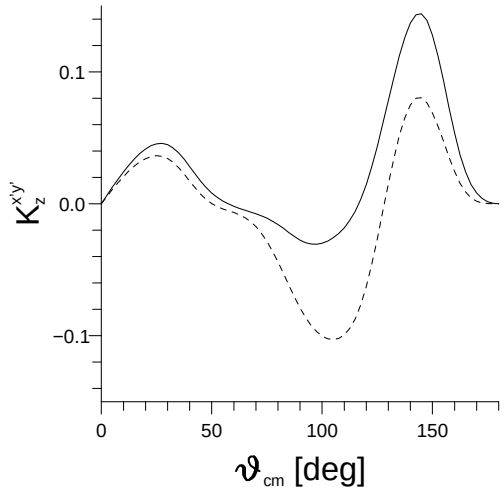

Fig. 18. This is the continuation of Fig. 2 towards higher energies. We see that the discrepancy between theory based on NN forces only and data increases. It reaches about 11 % at 300 MeV. In[53] we included the 3NF and found that about half of that discrepancy could be removed. Relativistic effects have to become also visible, and very first estimates are mentioned in[53] which might add another shift of about the right remaining amount.

Let us now turn first to elastic scattering. In Figs. 19 and 20 we show the angular distributions for pd elastic scattering at 65 and 135 MeV. The underprediction already seen in Fig. 5 is shown again. This also occurs at 135 MeV. If one adds the 3NF (without further adjustment) the theoretical prediction is shifted upwards, especially in the minimum, directly into the data. This can be fortuitous, but in any case the result is beautiful. We find similar results for the pd deuteron vector analyzing power $A_y(d)$ shown in Fig. 21 for $E_{lab} = 135$ MeV. Again the 3NF pushes theory right into the data. However this is only the beginning of investigating 3NF's, since a serious counterexample is shown in Fig. 22. Here the proton analyzing powers $A_y(p)$ in their minima are plotted against energy. While the NN force prediction alone underestimates the data above about 100 MeV the inclusion of the 3NF pushes theory upwards by far too much. A strong discrepancy can also be seen in the full angular distribution of $A_y(p)$ at the higher energies[70]. Obviously the spin structure of the 3NF is not yet understood. We hope that chiral perturbation theory will provide important help towards a systematic approach[41] of that new dynamical structure in the 3N Hamiltonian.

At low energies 3NF effects are clearly visible for scattering observables, which scale with the triton binding energy. A first prominent example is the doublet nd scattering length. It is strongly correlated to the triton binding energy and both agree with data in a similar fashion [71]. This correlation is known as Philipps line[72]. There are more observables which very likely scale with the triton binding energy, see e.g. Ref.[73], where it is shown that the spin transfer coefficient $K_y^{y'}$ shown in Fig. 11 scales with the triton binding energy and all the NN force predictions together with the individually tuned 3NF's coincide with each other and the data. More recent predictions[74] are the longitudinal and transversal asymmetries of the $\vec{n}\vec{d}$ total cross section. Their measurements would be important to test theory.

The effect of the TMF on A_y at low energies is tiny and does not solve the A_y-puzzle. Presumably we see 3NF effects of still unknown nature.

Finally we would like to show two examples of 3NF effects in spin observables for elastic nd scattering. In Fig. 23 the correlation coefficient $C_{x,xy}$ and in Fig. 24 the spin transfer coefficient $K_z^{x'y'}$ are displayed. In both cases the same 3NF model as before was used. The figures show that the effects are strong and precise data are necessary to obtain information about the spin structure of the present as well as newly developed 3NF's.

0.1.9. Outlook

Searching for a fundamental nuclear Hamiltonian has been a longstanding issue since the early days of nuclear physics. With the advent of supercomputers it is now possible to exactly solve the most simple ansatz for such a Hamiltonian based on realistic NN forces in light, bound nucleon systems and in three nucleon scattering. In both cases it was found that NN forces alone are not sufficient to provide the correct binding energies and level spacings in light nuclei [2] nor to find agreement with all three-nucleon scattering observables [1]. Therefore together with present day NN forces additional dynamical ingredients are needed, the most obvious ones are 3NF's. With respect to this new dynamical ingredient we are at present still at an early stage of insights. The 3NF of longest range is the 2π - exchange, and was formulated in the late 1970's[43]. Today modifications thereof are still made and presumably necessary[47]. This 2π - exchange force gives clear signals by improving the theorectical description of data in several cases. However, discrepancies still remain in other cases, which indicate that strength as well as spin- and isospin structure of 3NF's still need further exploration. Thereby very likely chiral perturbation theory will be of significant guidance [41]. In testing the nuclear Hamiltonian especially with respect to 3NF's it is very natural to study first 3N observables. Especially the break-up process can be expected to be **the** important source of information. It has the most detailed observables with three final nucleon momenta.However, its systematic experimental exploration has not started yet. Clearly this has to include the measurements of many spin observables. According to our present day insights energies above 100 MeV nucleon laboratory energy would be a promising place to perform the investigations.

At those higher energies relativistic effects will be visible and a relativistic generalization of the Schroedinger equation has to be developed [32]. The number of angular momenta increases rapidly in the energy regime up to the pion threshold (and higher), and it appears to us that proceeding without partial wave decomposition seems more appealing, both algebraically and in the numerical implementation. First steps can be found in [75].

The reliable control of 3N scattering is of great importance in the theoretical analysis of inelastic electron and photon scattering on ^{3}He [76]. The final state interaction can play an important role and neglecting it will obscure the view on the absorption process of the photon in the nuclear system to such an extent that the central issues, extraction of the electromagnetic nucleon form factors in a nuclear medium , probing mesonic exchange currents, testing wavefunction properties etc., can not be studied reliably. Corresponding results apply to other processes on ^{3}He like μ-capture or photon induced K Λ (K Σ) production, where final state interactions are very important. In the latter case the final state interaction among a hyperon and two nucleons is the central point of interest, since it will give information on the YN forces.

It might turn out that four-nucleon scattering probes nuclear dynamics even more sensitively. With the rapid increase of computer resources first exciting results found in 4N scattering [5] can be very likely brought to a full convergence and one will also have access to truly investigate the excited levels of the 4N systems, which are in reality resonances and thus belong to the 4N continuum.

Last not least the still pending problem of correctly including the pp Coulomb forces in few-nucleon scattering still sticks out and leaves a very uncomfortable theoretical uncertainty in the analysis of certain data. Right now a straight forward solution is not in sight.

Acknowledgments

I would like to thank my colleagues H. Witała, D. Hüber, H. Kamada and A. Nogga for a very enjoy-

able collaboration over many years and the John von Neumann-Institut for computing in Jülich providing the access to supercomputers.

References

1. W. Glöckle, H. Witała, D. Hüber, H. Kamada, J. Golak, Physics Reports 274, 107 (1996)
2. J. Carlson, R. Schiavilla, Review of Modern Physics 70, 743, (1998)
3. W. Glöckle, H. Kamada, Phys. Rev. Lett. 71, 1971 (1993)
4. M. Viviani, A. Kievsky. S. Rosati, Few-Body Systems 18, 25 (1995)
5. A. Fonseca, Phys. Rev. Lett. 83, 4021 (1999) and references therein
6. L.D. Faddeev, Mathematical Aspects of the three-body problem in quantum scattering theory (Davey, New-York 1965)
7. W. Glöckle, The Quantum-Mechanical Few-Body Problem, Springer Verlag, Berlin, Heidelberg 1983
8. W. Glöckle, Nucl. Phys. A141, 620 (1970)
9. H. Witała, Th. Cornelius, W. Glöckle, Few-Body Systems 3, 123 (1988)
10. A. Stadler, W. Glöckle, P.U. Sauer, Phys. Rev. C44, 2319 (1991)
11. W. Glöckle, Zeitschrift für Physik 271, 31 (1974)
12. D. Hüber, H. Kamada, H. Witała, W. Glöckle, Acta Phys. Polonica B28,1677 (1997)
13. L.L. Foldy, W. Tobocmann, Phys. Rev. 105, 1099 (1957)
14. G. Cattapan, V. Vanzani, Phys. Rev. C19, 1168 (1979)
15. B.A. Lippmann, Phys. Rev. 102, 264 (1956)
16. G. Bencze, C. Chandler, Phys. Lett. 90A, 162 (1982)
17. E.O. Alt, P. Grassberger, W. Sandhas, Nucl. Phys. B2, 167 (1967)
18. E.W. Schmidt, H. Ziegelmann, The Quantum Mechanical Three-Body Problem, Vieweg Tracts in Pure and Applied Physics, Vol 2 (1974)
19. G.O. Ohlsen, Rep. Prog. Phys. 35, 717 (1972)
20. M. Simonins, Lecture Notes in Physics 30, 38 (1973)
21. Madison Convention, Proc. Third Int.Symp. on polarization phenomena in nuclear reactions, Madison (1970), ed. H.H. Barshall and W. Haeberli, (Univ. of Wisconsin, Madison, 1971), p.XXV
22. C. Lovelace, in: Lectures of the 1963 Edinburgh Summer School, ed. R.G. Moorhouse (1964)
23. R. Aaron, R.O. Amado, Y.Y. Yan, Phys. Rev. 140, B 1291 (1965)
24. Y. Koike, J. Haidenbauer, W. Plessas, Phys. Rev. C 35, 396 (1987)
25. D. Hüber, H. Kamada, H. Witała, W. Glöckle, Few-Body Systems 16, 165 (1994)
26. D. Hüber, H. Witała, A. Nogga, W. Glöckle, H. Kamada, Few-Body Systems 22, 107 (1997)
27. W. Glöckle, G. Hasberg, A.R. Neghabian, Z. Phys. A305,217 (1982)
28. S.A. Coon, W. Glöckle, Phys. Rev. C23, 1790 (1981)
29. H. Witała, W. Glöckle, Th. Cornelius, Phys. Rev. C39, 384 (1989)
30. A. Stadler, Nucl. Phys. A631, 152c (1988)
31. J.L. Forest, V.R. Pandharipande, J. Carlson, R. Schiavilla, Phys. Rev. C52, 576 (1995)
32. B.D. Keister, W.N. Polyzou, Adv. Nucl. Phys. 20,225 (1991)
33. W.N. Polyzou, W. Glöckle, Few-Body Systems 9, 97 (1990)
34. R. Machleidt, Adv. Nucl. Phys. 19, 189 (1989)
35. V.G.J. Stoks, R.A.M. Klomp, C.P.F. Terheggen, J.J. de Swart, Phys. Rev. C49, 2950 (1999)
36. R.B. Wiringa, V.G.J. Stoks, R. Schiavilla, Phys. Rev. C51, 38 (1995)
37. R. Machleidt, F. Sammarruca, Y. Song, Phys. Rev. C53, R1413 (1996)
38. R. Machleidt, K. Holinde, Ch. Elster, Phys. Rep. 149, 1 (1987)
39. K. Holinde, Few-Body Systems, Suppl. 8, 448 (1995)
40. E. Epelbaum, W. Glöckle, U. Meissner, to appear in Nucl. Phys. A
41. D. Hüber, J.L. Friar, A. Nogga, H. Witała, U. van Kolck, nucl-th/ 9910034
42. J. I. Fujita, H. Miyazawa, Prog. Theor. Phys. 17, 360 (1957)
43. S.A. Coon, M.D. Scadron, P.C. McNamee, B.R. Barrett, D.W.E. Blatt, B.H.J. McKellar, Nucl. Phys. A317,242 (1979)
44. H.T. Coelho, T.K. Das, M.R. Robilotta, Phys. Rev. C28, 1812 (1989); M.R. Robilotta, H.T. Coelho, Nucl. Phys. A460, 645 (1986)
45. U. van Kolck, Phys. Rev. C49, 2932 (1994)
46. S.A. Coon, M.T. Peña, Phys. Rev. C48, 2559 (1993)
47. J.L. Friar, D. Hüber, U. van Kolck, Phys. Rev. C59,53 (1999)
48. J. Carlson, V.R. Pandharipande, R.B. Wiringa, Nucl. Phys. A401, 59 (1983)
49. J.A. Eden. M.F. Gari, Phys. Rev. C53, 1510 (1996)
50. A. Nogga, D. Hüber, H. Kamada, W. Glöckle, Phys. Lett. B409, 19 (1997)
51. K. Chmielewski. S. Nemoto, A.C. Fonseca, P.U. Sauer, Few-Body Systems, Suppl. 10, 235 (1999)
52. W. P. Abfalterer, F. B. Bateman, F. S. Dietrich, Ch. Elster, R.W. Finlay, W. Glöckle, J. Golak, R.C. Haight, D. Hüber, G.L. Morgan, H. Witała, Phys. Rev. Lett. 81, 57 (1998)
53. H. Witała, H. Kamada, A. Nogga, W. Glöckle, Ch. Elster, D. Hüber, Phys. Rev. C. 59, 3035 (1999)
54. E.O. Alt, A.M. Muhkamedzhanow, A.I. Sattarov, Few-Body Systems, Suppl. 10, 231 (1999)
55. W. Grüebler, V. König, P.A. Schmelzbach, F. Sperisen, B. Jenny, R.E. White, F. Seiler, H.W. Roser, Nucl. Phys. A398, 445 (1983)
56. H. Shimizu, K. Imai, N. Tamura, K. Nisimura, K. Hatanako, T. Saito, Y. Koike, Y. Taniguchi, Nucl. Phys. A382, 242 (1982)
57. J.E. McAninch, L.O. Lamm, W. Haeberli, Phys. Rev. C50, 589 (1994)
58. C.R. Howell, W. Tornow, K. Murphy, H.G. Pfützner, M.L. Roberts, Anli Li, P.D. Felsher, R.L. Walter, I. Slaus, P.A. Treado, Y. Koike, Few-Body Systems 2, 19 (1987)
59. H. Dobiasch, R. Fischer, B. Haesner, H.O. Klages, P. Schwarz, B. Zeitnitz, R. Maschuw, K. Sinram, W. Wick, Phys. Lett. B76, 195 (1978)
60. L. Sydow, S. Lemaitre, P. Niessen, K.R. Nyga, G. Rauprich, R. Reckenfelderbäumer, S. Vohl, H. Paetz gen. Schieck, Nucl. Phys. A567, 55 (1994)

61. J. Zejma, Phd thesis, Jagellonian University, Cracow 1995, unpublished
62. G. Rauprich, S. Lemaitre, P. Niessen, K.R. Nyga, R. Reckenfelderbäumer, L. Sydow, H. Paetz gen. Schieck, H. Witała, W. Glöckle, Nucl. Phys. A535, 313 (1991)
63. N. Sakamoto et al, Phys. Lett. B367, 60 (1996)
64. E. Stephenson, H. Witała, W. Glöckle, H. Kamada, A. Nogga, Phys. Rev. C60, 061001
65. A. Kievsky, Few-Body Systems, Suppl. 10, 27 (1999)
66. H. Witała, D. Hüber, W. Glöckle, Phys. Rev. C49, R14 (1994)
67. W. Tornow, H. Witała, A. Kievsky, Phys. Rev. C57, 555 (1998)
68. D. Hüber, J.L. Friar, Phys. Rev. C58, 674 (1998)
69. E. Gonzalez Trotter, F. Salinas, Q. Chen, A.S. Crowell, W. Glöckle, C.R. Howell, C.D. Roper, D. Schmidt, I. Slaus, H. Tang, W. Tornow, R.L. Walter, H. Witała, Z. Zhou, Phys. Rev. Lett. 83, 3788 (1999)
70. R. Bieber et al, to appear in Phys. Rev. Lett.
71. C. R. Chen, G.L. Payne, J.L. Friar, B.F. Gibson, Phys. Rev. C39, 1261 (1989)
72. G. Barton, A.C. Phillips, Nucl. Phys. A132, 97 (1969)
73. L. Sydow, S. Vohl, S. Lemaitre, H. Patberg, R. Reckenfelderbäumer, H. Paetz gen. Schieck, W. Glöckle, D. Hüber, H. Witała, Few-Body Systems 25, 133 (1998)
74. H. Witała, W. Glöckle, J. Golak, D. Hüber, H. Kamada, A. Nogga, Phys. Lett. B447, 216 (1999)
75. W. Schadow, Ch. Elster, W.Glöckle, to appear in Few-Body Systems
76. W. Glöckle in Proceedings of the Second Workshop on Electronuclear Physics with Internal Targets and the Blast Detector, eds. R. Alarcon, R. Milner, World Scientific 1999, page 185
77. A. Pickelsimer, R. A. Rice, R. Brandenburg, Few Body Systems 19,47 (1995)